A review of relaxation and structure in some turbulent plasmas: magnetohydrodynamics and related models

William H. Matthaeus[1], David C. Montgomery[2] Minping Wan[1], and Sergio Servidio[3]
[1] *Bartol Research Institute, University of Delaware, Newark, Delaware 19716, USA*
[2] *Department of Physics and Astronomy, Dartmouth College, Hanover, NH*
[3] *Dipartimento di Fiscia, Universita della Calabria, Rende, Italia*

A brief overview is provided as an introduction to hydrodyanamic-like turbulence that characterizes the dynamics of plasmas in several parameter regimes. This includes magnetohydrodynamics (MHD), the electron fluid plasma, which is closely related to two dimensional hydrodynamics, and the solar wind, which is usually viewed as a laboratory for three dimensional MHD, with more involved plasma physics at the dissipative scales. An emphasis is places on energy decay, spectra, relaxation processes, coherent structures and higher statistics with selected applications in solar wind, and laboratory plasmas.

I. INTRODUCTION

The scope of turbulence theory has broadened remarkably in the recent era. Technological advances have broadened the study of turbulence to a variety of systems while also motivating and enabling various applications. This breadth offers a great challenge in responding to the charge "to assess the achievements of the last 50 years of turbulence research and to identify future challenges that still remain" given to this Colloquium. The challenge is daunting even in the relatively limited context of the present review. Here some topics are reviewed in magnetohydrodynamic (MHD) turbulence, and its close relatives in plasma physics, such as Guiding Center Fluid or two-fluid (Hall) MHD. Experimental techniques, computing technology, remote sensing methods and *in situ* spacecraft observations have allowed ideas of MHD turbulence theory to deeply penetrate space physics, solar physics, astrophysics, cosmology laboratory plasma and fusion physics, geophysics and planetology, and numerous materials science and engineering applications. Recognizing the futility of engaging all of these subjects here, this review will focus on some advances that relate these new subjects to classical turbulence ideas, while touching on associated applications, mainly in the solar wind, the corona, and laboratory electron plasmas. In the conclusions section a brief and incomplete attempt will be made to point towards some important subjects that are entirely neglected here.

II. MODELS AND PHYSICAL QUANTITIES OF INTEREST

A plasma, described here as an electrically conducting gas or fluid, evolves in response to both mechanical and electromagnetic forces. To describe its dynamics in a simple way, one can begin with the momentum equation for hydrodynamics, and add a Lorentz force on the fluid elements. This depends on the low frequency magnetic field and the electric current density. The magnetic field can then be advanced in time through Faraday's law, with a closure based on Ohm's law. For simplicity, as in hydrodynamic turbulence, the focus is often on the constant density incompressible model, which provides an adequate context for the issues of MHD turbulence that are of primary concern here (see [15]). Ignoring compressible effects necessarily discards at the onset important and detailed features of the plasmas that MHD is intended to approximate. Nevertheless this is a quick way to arrive at the study of the nonlinear scale-to-scale couplings that are at the core of the turbulence problem. The problem of compressible plasma turbulence is much larger and is entirely outside the current scope apart from a few remarks below and in the conclusions.

The incompressible MHD model, in terms of the fluid velocity $\mathbf{u}$ and the magnetic field $\mathbf{B}$, involves the momentum equation

$$\frac{\partial \mathbf{u}}{\partial t} + \mathbf{u}\cdot\nabla\mathbf{u} = -\frac{1}{\rho}\nabla p + \frac{1}{4\pi\rho}(\nabla\times\mathbf{B})\times\mathbf{B} + \nu\nabla^2\mathbf{u} \quad (1)$$

and the magnetic induction equation

$$\frac{\partial \mathbf{B}}{\partial t} = \nabla\times(\mathbf{u}\times\mathbf{B}) + \mu\nabla^2\mathbf{B}. \quad (2)$$

The plasma density ρ, the kinematic viscosity ν, and the magnetic diffusivity μ, are assumed to be uniform constants. Therefore both the velocity and magnetic field are solenoidal, $\nabla\cdot\mathbf{u} = \nabla\cdot\mathbf{B} = 0$. The pressure p, as in incompressible hydro, provides a constraint that maintains incompressibility, and is determined by taking the divergence of Eq. (1). The dimensionless Reynolds number $R = uL/\nu$ (where u is a typical velocity and L a typical length scale) and magnetic Reynolds number $R_m = uL/\mu$ are measures of the relative strength of the non-linear terms and linear (dissipative) terms in the dynamical equations. Highly turbulent MHD occurs at high values of R and R_m.

We recall that MHD is frequently applied to space and astrophysical plasmas for which the derivation of the model is not so clear as one would like. This contrasts the more firm conceptual basis hydrodynamics or gas dynamics, which rests

either on macroscopic or perturbative (such as Chapman Enskog expansion) approaches given in standard texts on statistical mechanics. For plasmas with low collisionality, the basic structure of MHD emerges from conservation of mass, momentum and energy, along with the Maxwell-Ampere and Faraday laws, upon ignoring displacement current and adopting a suitable form of Ohm's law. However, in some applications there may not be a clear path to closing the system with a single isotropic pressure field, or a convincing calculation of viscosity, resistivity and other transport coefficients such as thermal conductivity. The study of the origin of dissipation in space and astrophysical plasmas leads to problems of great importance and difficulty, as does the investigation of the physics of the pressure tensor. Many topics relating to the kinetic physics of the solar wind have been studied extensively (see e.g., Marsch (2006) [77].) Equally difficult and important problems arise in connection with boundary conditions that might need to be imposed, as the number and type of imposed conditions will differ in plasma and fluid models.

A customary approach in numerical work is to employ scalar dissipation coefficients, with values based on numerical limitations of spatial resolution rather than on physical realism. For turbulent MHD this is justified in part by assuming that the nonlinear cascade is mainly from large to small scales, and the kinetic dissipation mechanisms act to absorb whatever energy arrives at small scales through spectral transfer. This is only partially satisfactory, and a more comprehensive theoretical understanding of the nature of dissipation in low collisionality MHD applications is desirable, though it may be neither simple in nature nor of universal form. On the optimistic side, when observations are available, e.g., for the solar wind [26], one sees a broad inertial range that separates energy-containing and dissipation ranges [68]. One can infer an effective Reynolds number for the solar wind in this way. Ignoring the difference between viscous and resistive dissipation, one might employ the hydrodynamic estimate of the dissipation wavenumber $k_d = (\epsilon/\nu^3)^{1/4}$. Using the Taylor-von Karman estimate of the decay rate $\epsilon = u^3/\lambda$, this can be cast in the form $k_d\lambda = R^{3/4}$, or $R = (k_d\lambda)^{4/3}$ where R is the Reynolds number. The quantity $k_d\lambda$ is approximately the bandwidth of the inertial range. Therefore for a three to four decades inertial range (e.g., the solar wind, approximately), one has $R \approx 10^5$ (see e.g., [152]. For the lower solar corona, a five to six decades inertial range is estimated, so $R \approx 10^8$. For such high Reynolds numbers, the MHD approximation becomes progressively better at the larger scales.

The energy is a quantity that focuses much attention in hydro and in MHD, because the nonlinear couplings in the fluid equations do not change its value, and therefore it is meaningful to speak of a "cascade" that exchanges energy among scales without changing the total amount present. In the high Reynolds number cascade there are many couplings that drive larger scale structures, and many that drive smaller scale structures. When there is a source of energy at large scales, and either dissipation (or for some other reason a deficit) of energy at small scales, then the latter class is dominant, sometimes by only a modest margin. This effect leads to a net transfer of energy from large to small scales. We will say more about this later. For now we call attention to a feature of MHD that distinguishes it from simple hydrodynamics– namely the potential presence of more than one cascade. This is caused by the fact that there is more one quadratic quantity that is preserved by MHD nonlinear couplings.

For homogeneous (periodic) incompressible MHD with zero mean magnetic field, there are three (known) ideal quadratic invariants: energy, $E = \langle |\mathbf{v}|^2 + |\mathbf{b}|^2 \rangle$, cross helicity $H_c = \langle \mathbf{v} \cdot \mathbf{b} \rangle$, and magnetic helicity $\langle \mathbf{b} \cdot \mathbf{a} \rangle$. Here $\mathbf{b} = \nabla \times \mathbf{a}$ and $\mathbf{a}$ is the magnetic vector potential. There is a lot more that can be said about the role of these additional invariants, and more will follow in sections below, but for now we note that the presence of as many as three conserved quadratic fluxes in an "inertial range" restricts the dynamics in important ways and gives rise to interesting effects such as inverse cascade, enhancement of nonlocal couplings and special properties of solutions such as 1/f noise. (In hydrodynamics there are two invariants – energy and kinetic helicity - but the latter is often viewed as of less importance than the additional ideal invariants of MHD. See [62].

The magnetic field may contain a uniform part $\mathbf{B_0}$ (below, the "DC magnetic field") or a smoothly varying part (which we identify as a local mean magnetic field) plus small scale fluctuations $\mathbf{b}$, that is $\mathbf{B} = \mathbf{B_0} + \mathbf{b}$. The large scale magnetic field supports propagation of hydromagnetic waves; here, for the incompressible case, we call these Alfvén waves [5, 6, 93, 111]. These waves are fluctuations transverse to the mean magnetic field, propagating along the mean magnetic field direction at the Alfvén speed $V_A = B_0/\sqrt{4\pi\rho}$.

Even the simplest MHD case, assuming incompressibility, isotropy, stationarity and homogeneity, is more complex than hydrodynamics. There are two distinct fields to deal with, the magnetic and velocity field, and additional complexity due to Alfvén wave propagation effects. There are at least two classes of timescales involved, the nonlinear time and the Alfvén crossing time. Moreover, the large scale magnetic field introduces a preferred direction and anisotropic effects on the fluctuations are present.

Here we arrive at a major difference between fluid and MHD turbulence. Unlike fluid turbulence, the nonlocal effect of large scales upon the small scales, described above as "sweeping," is an important issue for MHD turbulence. Beginning with the work of Iroshnikov (1964) and Kraichnan (1965) [57, 63], it has been argued that such effects play a significant role in MHD turbulence, even in the case of absent DC magnetic fields. If there is a strong, large-scale magnetic field, the small-scale fluctuations are subject to a sweeping-like effect due to Alfvén wave propagation. To discuss this it is useful to write MHD in a more symmetric form, in terms of the so-called Elsässer fields (Elsässer 1956), $\mathbf{z}_+ = \mathbf{u} + \mathbf{b}/\sqrt{4\pi\rho}$ and $\mathbf{z}_- = \mathbf{u} - \mathbf{b}/\sqrt{4\pi\rho}$

$$\frac{\partial \mathbf{z}_\pm}{\partial t} \mp \mathbf{V_A} \cdot \nabla \mathbf{z}_\pm = -\mathbf{z}_\mp \cdot \nabla \mathbf{z}_\pm - \frac{1}{\rho}\nabla P + \mu \nabla^2 \mathbf{z}_\pm, \quad (3)$$

where we have explicitly separated a term involving the large scale magnetic field (written here in terms of the Alfvén velocity $\mathbf{V_A}$). For simplicity, we assumed $\nu = \mu$. The total pressure $P = p + B^2/8\pi$ acts to enforce the constraints $\nabla \cdot \mathbf{z}_\pm = 0$.

Either $\mathbf{z}_+ = 0$ or $\mathbf{z}_- = 0$ provides exact solutions of the ideal MHD equations. The nonzero field is often said to correspond to *wave packets* that propagate along the mean field direction. This description can be misleading because the "packets" may not be localized, and also may not propagate. Non-propagating fluctuations with wavevectors strictly perpendicular to the mean magnetic field have zero phase speed. In any case, one sees from the MHD equations that both type of fluctuations $\mathbf{z}_\pm$ are needed for the nonlinear terms to be non-zero and sustain turbulence [38, 63].

Kraichnan (1965) noted that the mean magnetic field sweeps the small scale structures which interact and during that time non-linear transfer of energy between length scales occurs (in the Kraichnan picture the "wave packets" suffer brief "collisions" during which energy transfer occurs). One can see then that the mean magnetic field induces an inhibition of the nonlinear energy cascade (Chen and Kraichnan, 1997) [32].

For high Reynolds number MHD turbulent flows in astrophysical and space environments, there is scale separation to distinct physical processes at large and small scales. Specifically, one divides the dynamics into a small scale part that contains "small-small" and "large-small" couplings, and a large-scale part (see [1, 159], reminiscent of k-epsilon and other hydrodynamic turbulence modeling approaches [73]. This type of "turbulence transport theory" generalizes WKB theory for MHD and plasma waves [6, 52], and has proven useful in mapping turbulence amplitudes across large distances within the corona and heliosphere [20, 158]. Adaptations of transport theory can apparently help explain both the origin of the solar wind [34, 149] and the highly nonadiabatic profile of temperature throughout the interplanetary medium [21, 35]. Due to space and time limitations, we will not review transport theory further below, but concentrate on theories of homogeneous and/or local processes in MHD turbulence and its relatives.

III. ENERGY DECAY

A central result of turbulence theory is the similarity decay of energy (per unit mass) for the free decay problem [58]. For moderate to high Reynolds numbers the rate of decay of energy become independent of the viscosity, and governed by the action of the large scale eddies. The basic physical content of this simplest turbulence phenomenology is captured in the equations for decay of energy per unit mass U^2 and the similarity length scale L, namely

$$\frac{dU^2}{dt} = -\alpha \frac{U^3}{L}; \qquad \frac{dL}{dt} = \beta L. \tag{4}$$

During similarity decay of isotropic turbulence the correlation functions are stretched and recalled according to

$$R(r) = U^2(t)\hat{R}(r/L(t)) \tag{5}$$

For MHD the analogous development proceeds by forming the two point correlation functions of the Elsässer fluctuations, and examining the conditions for a similarity solution [151]. For globally isotropic MHD turbulence (lacking an imposed DC magnetic field), the consistency conditions for a similarity solution, in terms of Elsässer energies Z_+^2 and Z_-^2 and associated length scales L_+ and L_-, are

$$\frac{dZ_+^2}{dt} = -\alpha_+ \frac{Z_+^2 Z_-}{L_+}; \qquad \frac{dZ_-^2}{dt} = -\alpha_- \frac{Z_+ Z_-^2}{L_-} \tag{6}$$

$$\frac{dL_+}{dt} = \beta_+ Z_-; \qquad \frac{dL_-}{dt} = \beta_- L_+ \tag{7}$$

where $\alpha_\pm$, $\beta_\pm$ are constants. Note that these equations require two distinct length scales $L_+ \neq L_-$ whenever the cross helicity is non zero and $Z_+ \neq Z_-$.

When a DC magnetic field is present and the fluctuations are assumed to be axisymmetric about this direction, one allows in principle at least four characteristic lengths L parallel $\parallel$ and perpendicular $\perp$ for both $+$ and $-$ fluctuations. One finds that additional restriction need to be imposed to find a similarity solution. One solution is that the parallel and perpendicular length scales remain in constant proportion to one another for all relevant time scales, that is $L_+^\parallel / L_+^\perp = q_+$, and $L_-^\parallel / L_-^\perp = q_-$, for constants $q_\pm$.

These requirements for similarity decay hint at nonuniversal properties of MHD turbulence because ratios such as L_+/L_- and $q_\pm$ can apparently take on any value. This leads in principle to many types of MHD turbulence. More discussion on this will appear below. Note that even if there is not a universal decay law, there still may be interesting families of similarity decay. It's just that having more than one cascaded quantity complicates the picture. Similarity decay in 3D MHD has been examined in simulations [15, 55], but usually employing only one length scale. The impact of multiple dimensionless parameters, and multiple cascades, complicates MHD and can cause us to question whether "universality" remains a useful concept (see [151]), but this remains an open and hotly discussed issue.

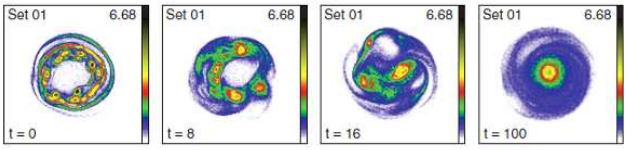

FIG. 1: Vorticity images showing evolution of Penning trap data. (Rodgers et al., PRL, 2010)

On the narrower question of existence of similarity decay laws, it is interesting to note that an analogous situation occurs in 2D hydrodynamics, where energy $E = \langle u^2 \rangle$ and enstrophy $\Omega = \langle |\nabla \times \mathbf{u}|^2 \rangle$ are both inviscid quadratic invariants, and both a direct and inverse cascade are possible [65]. This leads to interest self organized behavior in the long time limit of decay, which will be discussed further below in Section VI . Here show some evidence that this type of system can engage in a similarity decay of the direct cascaded quantity – in this case enstrophy Ω. The system in question is a Penning trap containing a pure nonneutral electron plasma, operating

in a parameter range in which the cyclotron frequency is much large than the plasma frequency. In this regime the equation of motion for the coarse grained number density of electrons is identical to the vorticity equation in 2D hydrodynamics. Meanwhile, since the $E \times B$ drift velocity is divergenceless, and the electric potential due to the electron charges obeys a Poisson equation, there is an almost complete analogy between the fluid scale electron motions in the Trap, and the equations for a 2D incompressible fluid in a circular container. See [39].

To a reasonable degree of approximation, the electron density $n(r, \theta, t)$ follows 2D, z-averaged, $\mathbf{E}\times\mathbf{B}$ drift motion [39], where

$$\mathbf{v}_D = -\frac{c\nabla\phi \times \hat{\mathbf{z}}}{B}, \quad \nabla^2\phi = -4\pi|e|n, \tag{8}$$

where ϕ is the electrostatic potential and $\mathbf{E} = -\nabla\phi$. For this system, $\mathbf{v}_D$ is equivalent to the 2D fluid velocity $\mathbf{v}$, with the vorticity ω proportional to electron number density n, and stream function ψ proportional to $-\phi$ the potential. Because of this analogy, the evolution of the system is governed by the 2D NS equation for one-sign vorticity,

$$\frac{\partial\omega}{\partial t} + (\mathbf{v}\cdot\nabla)\omega = \nu\nabla^2\omega, \tag{9}$$

where $\mathbf{v} = \nabla\psi \times \hat{\mathbf{z}}$ and $\nabla^2\psi = -\omega$. The term involving viscosity ν is familiar in hydrodynamics but not well motivated in the guiding center plasma case, as the dissipation mechanisms may differ significantly in NS and MPT [67].

The three dimensionality of the real experiment must be neglected, and differences between the nonideal effects in the electron plasma and 2D hydro must be neglected. Interestingly [123] good agreement is found in comparing 2D hydro simulations and Penning Trap data (see Fig 1) when the boundary conditions in the simulation are chosen to be free-slip, even though there is viscous diffusion in the interior. This boundary condition corresponds to a perfect conductor, having constant potential.

Fig 1 shows important features of 2D hydro that also are analogous to features of MHD in both 2D and 3D. In particular, one see the simultaneous formation of large scale coherent structures that persist for long times, and the small scale features of the cascade including small scale (presumably) dissipative structures. In 2D hydro the observed transfer to large scales is an inverse transfer of energy. The direct transfer to small scale is an *enstrophy cascade*. In 2D MHD the inverse transfer is that of mean square magnetic potential [43–45] and the direct cascade is an energy cascade. In 3D MHD the direct cascade is again of energy, and when magnetic helicity if present there can be an inverse cascade. The behavior of cross helicity is intermediate (see [141]).

If we assume a similarity decay for 2D hydrodynamics or for the Penning trap system, then it is possible to state a modified decay law that turns out to work reasonably well. The needed modification is based on the recognition that much of the vorticity distribution is somehow "destined" to be locked up in the long-lived metastable state that is eventually achieved in Penning trap relaxation (see Section below). Suppose this metastable state has an enstrophy Ω_{ms}. If one removes Ω_{ms} from budget of enstrophy that has impact on the direct cascade, then a similarity law can be written for the remaining "free enstrophy" Ω^{F}or excess above this long term value [124]. To continue, assume that the global enstrophy decay timescale τ depends only on $\Omega^{\mathrm{F}}$and a characteristic length scale l. The only dimensionally consistent choice is $\tau = 1/\sqrt{\Omega^{\mathrm{F}}}$. This is analogous to $\tau = l/\sqrt{E}$ in 3D, where l is a correlation length. Then free enstrophy changes in time according to $d\Omega^{\mathrm{F}}/dt = -a\,\Omega^{\mathrm{F}\,\frac{3}{2}}$. for which the solution is:

$$\frac{\Omega^{\mathrm{F}}}{\Omega_0^{\mathrm{F}}} = \left(1 + 2\,a\,\sqrt{\Omega_0^{\mathrm{F}}}(t - t_0)\right)^{-2}, \tag{10}$$

Here $\Omega_0^{\mathrm{F}} = \Omega^{\mathrm{F}}(t_0)$ is the initial free enstrophy. For an initially disordered fluid with large Ω_0^{F}, 10 gives $\Omega^{\mathrm{F}} \sim t^{-2}$ for $a\sqrt{\Omega_0^{\mathrm{F}}}t \gg 1$, as in the isotropic case predicted by Batchelor [7]. The conditions for turbulence to be of sufficient strength to justify a similarity law such as Eq. (III) are not entirely clear, although large $\Omega_0^{\mathrm{F}}/\Omega_{ms}^{\mathrm{F}}$ would seem favorable.

Fig. 2 shows a test of the proposed similarity decay or free enstrophy, employing data from the University of Delaware Penning trap [92]. The final metastable state enstrophies for each experimental runs were used to compute Ω_{ms}, in terms of which the free enstrophy was computed. A variety of different experimental initial conditions were used in the comparison. It is apparent that the similarity decay of free enstrophy is a reasonable hypothesis for these datasets. This is encouraging with regard to extending the von Karman-Howarth analysis to more complex systems involving more than one cascaded quantity, such as MHD in 2D and helical MHD in 3D.

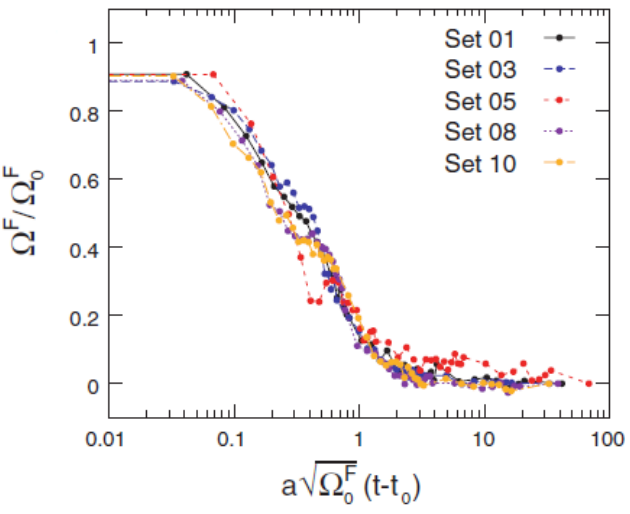

FIG. 2: Scaled free enstrophy versus adjusted nonlinear time. (Rodgers et al., PRL, 2010)

IV. SPECTRA AND VARIABILITY

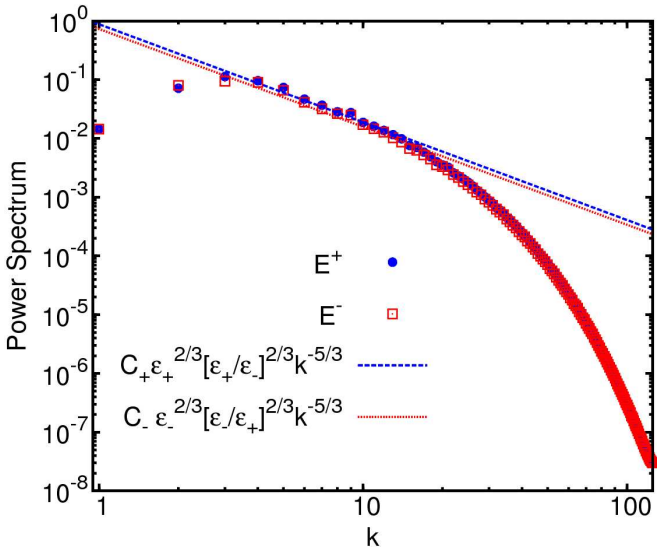

FIG. 3: Elsässer energy spectral densities E^+ (blue bullets) and E^- (red open squares) as a function of the wavenumber k. The dashed lines represents (see text) $E^{\pm} = C_{\pm}\epsilon_{\pm}^{2/3}[\epsilon_{\pm}/\epsilon_{\mp}]^{2/3}k^{-5/3}$, for $C_{\pm} = 2$, $\epsilon_+ = 0.26$ and $\epsilon_- = 0.24$ [130].

Probably the most famous result from classical hydrodynamic turbulence theory is the inertial range spectrum in which the omnidirectional energy is distributed across a wide range of (inertial range) wavenumbers k with a powerlaw spectrum varying as $k^{-5/3}$. For hydrodynamic turbulence in the inertial range the only important timescale is the local nonlinear time $\tau_{nl} = (ku_k)^{-1}$ for wavenumber k and u_k the contribution to the speed from excitations near k. Then the energy decay rate can be written $\epsilon \sim u_k^2/\tau_{sp}$, for spectral transfer time τ_{sp}. However here the only choice is $\tau_{sp} = \tau_{nl}$, so using $u_k^2 = k\mathcal{E}(k)$ for omnidirectional energy spectrum $\mathcal{E}$, one finds the Kolmogorov spectrum $\mathcal{E}(k) = C\epsilon^{2/3}k^{-5/3}$.

For MHD the situation is complicated by the multiplicity of available time scales, thus rendering ambiguous the spectral transfer time, which could, for example, depend on both nonlinear time and Alfvén time. For zero cross helicity let us designate the amplitude at k as $Z_k = Z_{k+} = Z_{k-}$, and write the large scale magnetic field as B_0. This may be either externally applied, or $B_0 \sim Z$ if it is due to the large scale fluctuations themselves. Then for the Kolmogorov-like theory of isotropic MHD, one chooses $\tau_{sp} = \tau_{nl}$ as in the hydro case, and the Kolmogorov spectrum is reproduced with $\mathcal{E}(k) = C\epsilon^{2/3}k^{-5/3}$ being the omnidirectional spectrum of the total incompressible energy. The theory of Kraichnan [63] supposes that the k-independent transfer of energy ϵ must be in direct proportion to the triple lifetime. Then $\epsilon = \tau_3(k)[\mathcal{E}(k)]^2k^4 = \tau_3(k)Z_k^2/\tau_{nl}^2(k)$. One notices here that the spectral transfer time in principle differs form the nonlinear time, and must involve the lifetime of the triple correlations. Kraichnan chooses the triple lifetime to be the Alfvén time $\tau_3(k) = \tau_A(k)$. From this it transpires that the energy spectrum is $\mathcal{E}(k) = C_{Kr}\epsilon^{1/2}B_0^{1/2}k^{-3/2}$. Pouquet et al [116] made the important observation that the Alfvén time may be due to a uniform large scale field or else the large scale magnetic fluctuations, which have a similar influence on much smaller scale inertial range fluctuations.

For finite cross helicity, $Z_k^+ \neq Z_k^-$. For this case and assuming a Kolmogorov like spectral theory, the development only involves the local nonlinear times scales $\tau_{nl}^{\pm}(k)$. Then (see [63, 160]) one finds that $\epsilon^{\pm} = C^{\pm}(Z_k^{\pm})^2/\tau_{nl}^{\pm} = C^{\pm}k(Z_k^{\pm})^2Z_k^{\mp} = C^{\pm}k^{5/2}E^{\pm}(k)\sqrt{E^{\mp}(k)}$. From these two relations we conclude that the steady Kolmogorov-like high Reynolds number MHD energy spectra are $E^{\pm}(k) = C_{\pm}\epsilon_{\pm}^{2/3}[\epsilon_{\pm}/\epsilon_{\mp}]^{1/3}k^{-5/3}$. Thus, the nonlinear time scales in the steady inertial range, can be written as $\tau_{nl}(k) \sim [C_{\pm}^{1/2}\epsilon_{\pm}^{1/3}[\epsilon_{\pm}/\epsilon_{\mp}]^{1/6}k^{2/3}]^{-1}$. We note that the Elsässer energy spectra shown in Fig. 3 admit a range of wavenumbers in which the spectral form is roughly varies in accord with a $k^{-5/3}$ behavior. Such wavenumber spectra are consistent with local scale to scale transfer dominated by nonlinearity and strain. However the physics of time decorrelation is distinct and may still depend on other effects and therefore other available MHD time scales.

One example is the advection (or sweeping) characteristic time at scale $1/k$, which may be expressed as $\tau_{sw}(k) \sim (ku_{rms})^{-1}$. Here the root-mean-square turbulent velocity $u_{rms} = \langle|\mathbf{u}|^2\rangle$ is a global quantity that is typically dominated by contributions from the large scales. Analogously, a characteristic Alfvèn time (averaged over direction, see [63]) can be defined as $\tau_A(k) \sim (kb_{rms})^{-1}$. [163] The root-mean-square magnetic field b_{rms} could in principle include contributions from both the fluctuations as well as a mean (uniform or very large scale) magnetic field. For the simulation employed here, b_{rms} is due only to fluctuations, which are assumed to have an isotropic distribution. It is worthy of note that the sweeping and Alfvénic propagation time scales both vary as $\sim k$. Finally, the viscous dissipation time is defined as $\tau_d \sim (\nu k^2)^{-1}$. In the inertial region, for reasonably small values of ν, both sweeping and eddy-turnover times are much smaller than the diffusive time. The wavenumber λ_d at which the dissipation and nonlinear times are equal, $\tau_{nl}(1/\lambda_d) = \tau_d(1\lambda_d)$, denotes the termination of the inertial range, and serves to define the Kolmogorov dissipation scale λ_d. Generally speaking in high Reynolds number turbulence, and for wavenumbers k in the inertial range, we expect an ordering such that $\tau_{nl}(k) > \tau_{nl}^{\pm}(k) > \tau_{sw}(k) \simeq \tau_A(k) > \tau_d(k)$. Indeed such ordering allows among other things, the possibility of a quasi-equilibrium properties within the inertial range.

The topic of the "correct" inertial range powerlaw index for MHD turbulence is another perennially discussed hot topic. The ambiguity between Kolmogorov $-5/3$ and Kraichnan $-3/2$ scaling is often debated, and to some extent the dichotomy can be resolved simply by allowing the lifetime of the triple correlations to be a composite of several effects [116], so that

$$\frac{1}{\tau_3(k)} = \frac{1}{\tau_{nl}(k)} + \frac{1}{\tau_A(k)} + \dots . \tag{11}$$

Indeed, using just the Alfvén and nonlinear time contributions

to τ_3 one can find a "spectral law" that interpolates neatly between $-5/3$ and $-3/2$ as the ratio of these two effects varies.

In the discussion of energy spectra it is traditional to appeal to examples. As we will presently see, this is not necessarily reliable. Nevertheless at this point it is worthwhile to illustrate that the observed wavenumber spectrum of magnetic fluctuations in the solar wind sometimes presents a very nice picture. Fig. 4 shows an example of the one dimensional trace magnetic field spectrum computed from an interval Voyager 2 data [79]. It is probably fair to say that this spectrum is "somewhat typical" and lies close to the $5/3$ prediction. The velocity field spectrum is often a little different [112], which is implied by the nonconstant Alfvén ratio $E_v(k)/E_b(k)$ [79]. Of course the steady spectral prediction, assuming local transfer and ignoring intermittency (see [125]) pertains only to the ideally conserved flux of *total energy*, $u^2 + b^2$ so this disparity of not of essential concern. Furthermore the exchange of energy between velocity and magnetic field is known to be highly nonlocal [1].

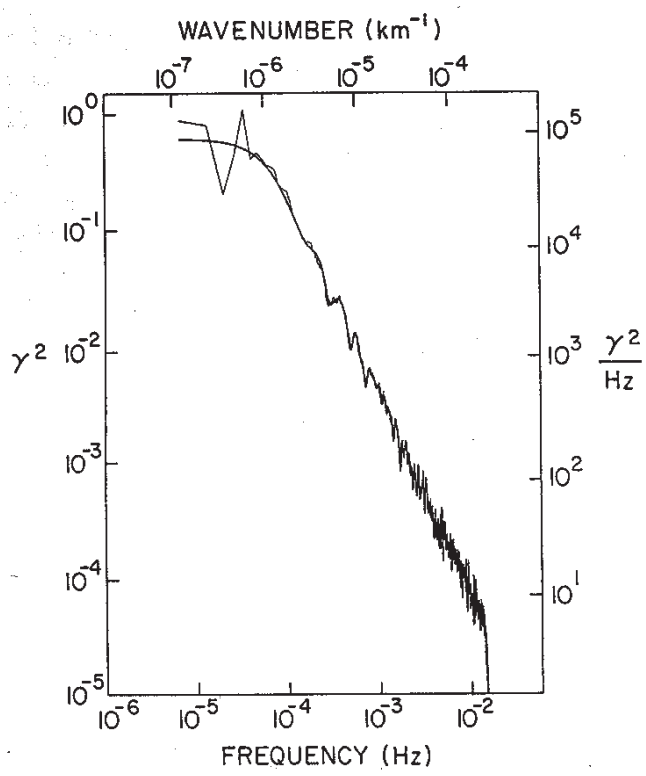

FIG. 4: Magnetic energy spectrum from Voyager 2 data, taken from Matthaeus and Goldstein (1982). The spectral slope is very close to $-5/3$.

Unfortunately, the solar wind is not so cooperative in presenting a single picture that one can claim evidences universality of one theoretical formulation. For example Vasquez et al [146] computed wavenumber spectra using Taylor hypothesis from 960 intervals of single spacecraft magnetic field data measured by the ACE spacecraft. The apparent inertial range spectra were fitted with a powerlaw $\sim f^{-q}$ in the (spacecraft frame) frequency range of 8 mHz to 0.1 Hz. The interval length used is one to several hours. The typical correlation scale [83] is about 10^6 km, which corresponds to about 40 minutes using a 400 km/s typical solar wind speed. Therefore the intervals used in the of the Vasquez et al study are a few correlation lengths in duration and should be long enough to obtain good estimates of the spectral index, with some spread due to finite sample size. The distribution of spectral indices q so obtained are showing in a histogram, reproduced here in Fig (5). One see that the distribution is approximately centered on the Kolmogorov value of 1.67, but also substantially overlaps with the 1.5 Kraichnan-Iroshnikov value. and has a half-width that includes values from about 1.4 to 1.8.

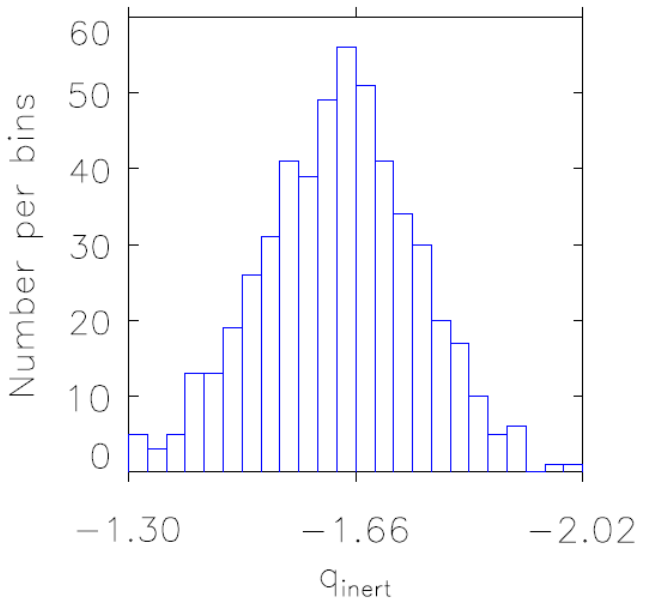

FIG. 5: Histogram of the slope of the energy spectrum from solar wind data at 1 AU. (Vasquez et al., JGR, 2007)

Of course the solar wind is not a controlled experiment, so some of this observed variation of spectral index may be from transient events, variations and nonsteady conditions, or even non-MHD effects. Another possibility, that variation of q is due to anisotropy, is discussed below in the following section.

In contrast to the solar wind observations, computer simulation provide controlled experiments. Nevertheless, the conditions imposed in simulations can differ in subtle ways according to variations in approach, including diverse forcing functions, boundary conditions, initial conditions, ratios of length scales, etc. Another major factor is the presence and strength of an applied uniform magnetic field. All of these can influence results on the spectral distributions and inertial range spectral indices obtained in simulation. This point was emphasized in a striking way in a recent paper by Lee al [72]. In this study, three simulation results in 3D MHD are contrasted, each starting from approximately the same global energy, cross helicity and magnetic helicity, and having the same Reynolds numbers. Even the energy spectra are very similar, each initial condition being an MHD generalization of the Taylor Green vortex. When the simulations are analyzed at the

time of peak dissipation, the results show very different spectra, k-dependence of Alfvén ratio, and other parameters such as the ratio of Alfvén to nonlinear times. The compensated total energy spectra are shown for these three runs, reproduced from the Lee at al paper [72].

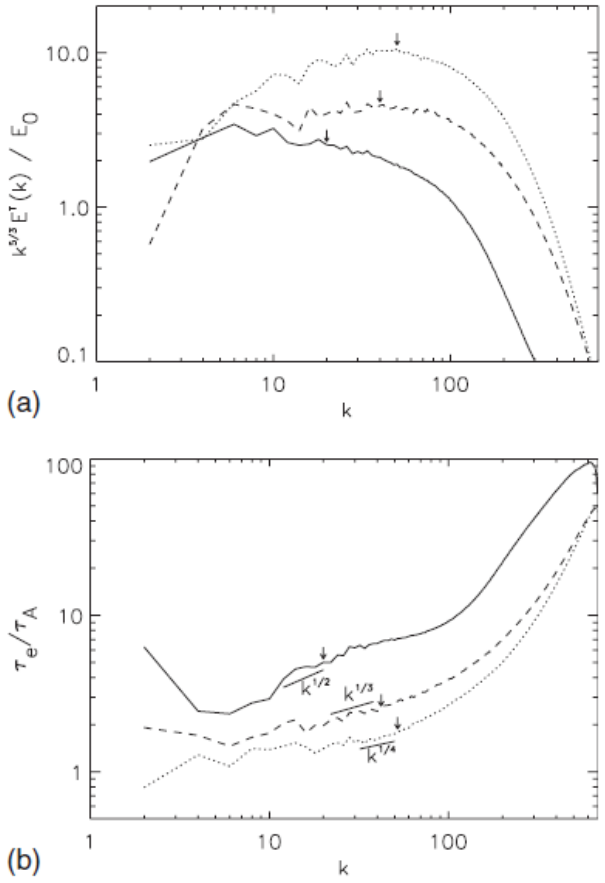

FIG. 6: Total energy spectra (a) compensated by $k^{5/3}$ and averaged over $\delta t = 0.5$ (1.52 turnover times) about the maximum of dissipation and ratio of nonlinear to Alfvén time scales as a function of wave number (b) for three runs from different initial fields but with the same initial energy spectra. Slopes are given only as a reference. The three arrows indicate the magnetic Taylor scale. Note that the three spectra follow noticeably different spectral laws and possibly different scale dependence for their time scales as well. (Lee et al., PRE, 2010)

The kind of variability seen in the above solar wind and simulation results suggest that MHD turbulence may be rather more variable than hydrodynamic turbulence. The problem with variability runs even deeper for "inverse cascade systems" such as 2D hydro, 2D MHD, 3D MHD, the Penning trap electron plasma, and similar systems. This is because such systems have a strong tendency to accumulate excitations in a only a few of its degrees of freedom, thus setting up a system that through enhancements of nonlocal interactions, can generate low frequency $1/f$ noise [36]. This type of scale invariant noise is particularly frustrating to practical attempts to uncover typical or average behavior. Systems with $1/f$ noise have long time tails on temporal correlation functions that thwart attempts to invoke the classical ergodic theorem in estimating ensemble averages though time integration. Interestingly, this feature seems to be absent in homogeneous hydrodynamic turbulence, but is present in systems that admit quasi-invariants, thus emulating temporarily the properties of systems that are strictly multiple ideal invariant inverse cascade systems [37, 91]. It is of interest that $1/f$ noise is observed in dynamo experiments and in the solar wind [84, 115].

V. ANISOTROPY

As mentioned in the introduction, the mean magnetic field imposes a preferred direction on MHD turbulence that cannot be removed by a Galilean transformation [63]. One of the associated effects, recognized long ago in laboratory plasma devices [122, 161] is the generation of fluctuations that maintain stronger correlation along the magnetic field than perpendicular to it. This effect was simulated first in 2D MHD [132], and later in 3D [110]. These studies showed that spectral transfer is unimpeded in the perpendicular direction in $k-$space, but is suppressed in the parallel direction. Nonlinear couplings that pump energy to smaller scales having larger perpendicular gradients are relatively unaffected by wave propagation effects. On the other hand, couplings that produce stronger parallel gradients are suppressed by Alfvén wave-like couplings that become ever stronger as the mean field strength is increased. This reasoning led to a rederivation of the equations of Reduced MHD (RMHD) [139] using an expansion in a small parameter that is in effect $\epsilon = b/B_0$ [98] for r.m.s. fluctuation strength b Order one nonlinear couplings are found to occur for values of parallel wavenumber satisfying $k_\parallel < \epsilon k_\perp$. Thus strong RMHD couplings occur when the large scale perpendicular Alfvén time $1/(bk_\perp)$ is less than the parallel Alfvén time $\tau_A(k_\parallel)$, or $bk_\perp > B_0 k_\parallel$ [156]. Later Goldreich and Sridhar [47] in effect refined this condition by employing the local nonlinear time $\tau_{nl}(k) = 1/(b_k k_\perp)$ instead of the transverse Alfvén time $1/(bk_\perp)$, and assuming steady state turbulence. The marginal condition for RMHD then becomes $b_k k_\perp \sim B_0 k_\parallel$, which is known as "critical balance."

Independent of details, all of the above experimental, theoretical and simulation results point towards the preference of MHD turbulence to excite more strongly those fluctuations that have stronger perpendicular, rather than parallel, gradients.

Evidence has also been accumulating that the solar wind contains a strong admixture of fluctuations that are in the above sense, quasi-two dimensional. There a number of ways that solar wind anisotropy can be measured. One approach [81] is to measure a large number of two point correlation functions (employing the Taylor hypothesis) at 1AU, with the radial direction, along which the observations are made, varying from interval-to-interval relative to the mean magnetic field direction. After accumulating the estimates, assuming axisymmetry about the mean field, and averaging, the result is the so-called Maltese cross correlation, shown in Fig 7. This

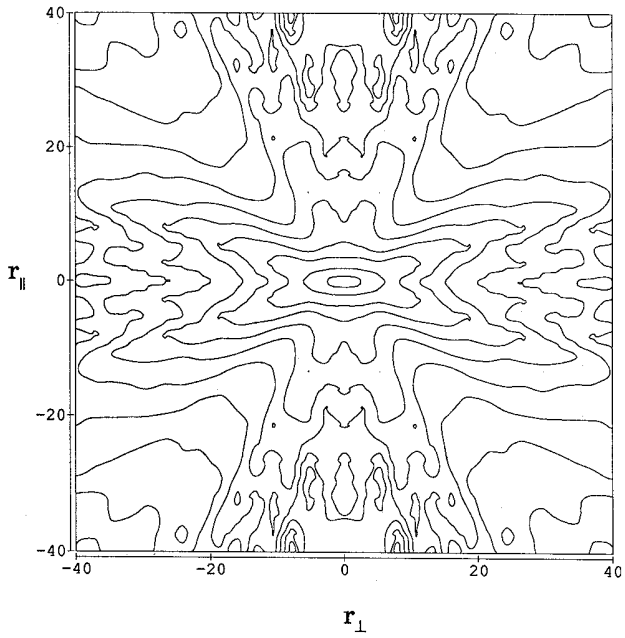

FIG. 7: Two point autocorrelation of the magnetic field $\mathbf{b} \cdot \mathbf{b}'$ as a function of coordinates parallel, and perpendicular, the mean magnetic field (axisymmetry assumed) in the solar wind at 1AU from $\approx$ 600 days of ISEE-3 data. (From [81]).

observation led to use of a "two component model" for solar wind fluctuations that no only proved useful in scattering theory and observations [12, 131] but also led to direct observational tests of anistropy [13] which confirmed that this parameterization of anisotropy corresponds reasonably well to observed solar wind properties. It is also interesting that considerations of the low Mach number approach to incompressibility in MHD at low to moderate plasma beta (thermal pressure over magnetic pressure) gives rise in a natural way to geometrical restrictions that correspond directly to the the two component model [157].

VI. GLOBAL RELAXATION

It has been recognized for quite some time that the magnetic field plays a special roles in electrodynamics, leading the possibility of global relaxation processes that favor special final states (e.g., [31, 153, 162]). This approach gained favor in the 70's when Taylor [142, 143] offered a physically motivated explanation for relaxation to force free states in Reversed Field Pinch experiments, often regarded, along with spheromaks [23] as the canonical laboratory devices for observation of MHD activity. This revival of relaxation theory occurred almost simultaneously with the description of inverse cascade in 3D MHD, driven by finite magnetic helicity [41]. The inverse cascade phenomenon in driven MHD is associated with the requirement that the nonlinear couplings must simultaneous conserve two ideal invariants, the energy E and magnetic helicity H_m. In analogy to its 2D hydrodynamic antecedent [64], transfer of turbulent excitation to higher wavenumber is accompanied by a concomitant transfer to lower wavenumbers, in order to simultaneously respect both conservation laws.

It is possible to establish the possibility of inverse cascade in a system such as 3D MHD by appeal to the absolute equilibrium Gibbs ensemble for an ideal Fourier Galerkin representation of the system, having a finite number of degrees of freedom, and exact set of quadratic conservation laws, and a Liouville theorem for maintenance of the canonical Gibbsian distribution [41, 64, 71, 128, 140]. When "Bose condensation" of a quantity into the longest allowed wavelength modes occurs for the Galerkin system as its number of included modes tends towards infinity, this is taken to be indicative of an inverse cascade for the corresponding driven dissipative system. This activity has led to identification of inverse cascades in 2D hydro, 3D MHD, 2D MHD, 3D Hall MHD, drift wave turbulence, and other systems.

Adaptation of the same physical reasoning to the case of decaying turbulence, leads to a set of *selective decay* principles [16, 78, 96, 97] that describe potential relaxed states of an MHD turbulent system. Schematically, if A is an inverse cascaded quantity and E a direct cascade quantity, then the selective decay principle predicts that spectral transfer leads to minimization of the ratio E/A, subject possibly to auxiliary constraints, and often limited by allowed eigenmode structure (i.e., geometry). Selective decay is a broad dynamical relaxation principle that accounts for behavior such as Taylor relaxation and the tendency for 2D MHD and hydro to evolve towards states characterized by long-lived large scale structures.

Searching for numerical evidence in MHD in support of selective decay led to the realization that there can be competing relaxation processes in MHD turbulence. Selective decay involves the energy and the magnetic invariant, but what about the third invariant, the cross helicity H_c?

It has been long known that minimizing energy subject to constant H_c leads to what are sometimes called large amplitude Alfvén waves, or "Alfvénic states" [5, 6, 93, 111]. Note that here familiar Alfvénic units are used. For incompressible MHD these states are described by $\mathbf{v} = \mathbf{b}$ at all points in space, or $\mathbf{v} = -\mathbf{b}$ at all points. These states (if permitted by boundary conditions) persist for all time in the absence of dissipation, as they lead to a full cancellation of the nonlinear terms. The same solutions survive if a uniform mean magnetic field $\mathbf{B}_0$) is added to the fluctuation $\mathbf{b}$; for that case the solutions propagate either along ($\mathbf{v} = -\mathbf{b}$) the $\mathbf{B}_0$ direction, or antiparallel to it $\mathbf{v} = -\mathbf{b}$).

Large amplitude Alfvénic states are in fact one of the defining characteristics of observed solar wind turbulence and are frequently observed [8–11, 24, 26], especially in the inner heliosphere. A classic example of Alfvénic turbulence in the solar wind from the Belcher and Davis paper is shown in Fig (8).

Based on the special position occupied by Alfvénic solutions, and their observation in space, Dobrowolney, Mangeney and Veltri [38] predicted that these states should emerge dynamically from MHD turbulence. This was verified in closure

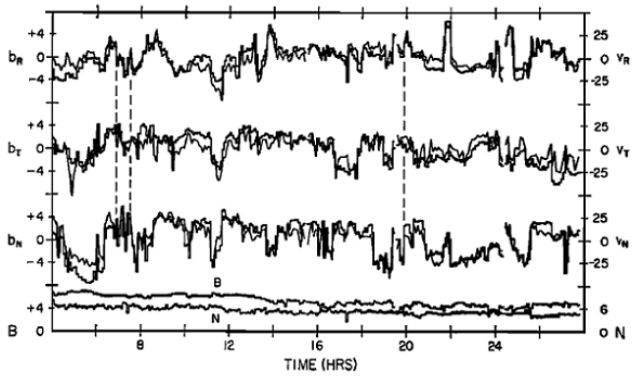

FIG. 8: Twenty-four hours of magnetic field and plasma data demonstrating the presence of nearly pure Alfvén waves. The upper six curves are 5.04-min bulk velocity components in km/sec (diagonal lines) and magnetic field components averaged over the plasma probe sampling period, in gammas (horizontal and vertical lines). The lower two curves are magnetic field strength and proton number density. (Belcher & Davis, JGR, 1971).

theory [48], and subsequently seen to emerge from turbulence evolution in 3D simulations [117] and in 2D simulations [80]. It is interesting to note that Alfvénic states appear to emerge from a *dynamic alignment* process that can be globally described by minimizing E for a specified H_c, or minimizing $\langle \mathbf{u}^2 + \mathbf{b}^2 \rangle / \langle \mathbf{u} \cdot \mathbf{b} \rangle$

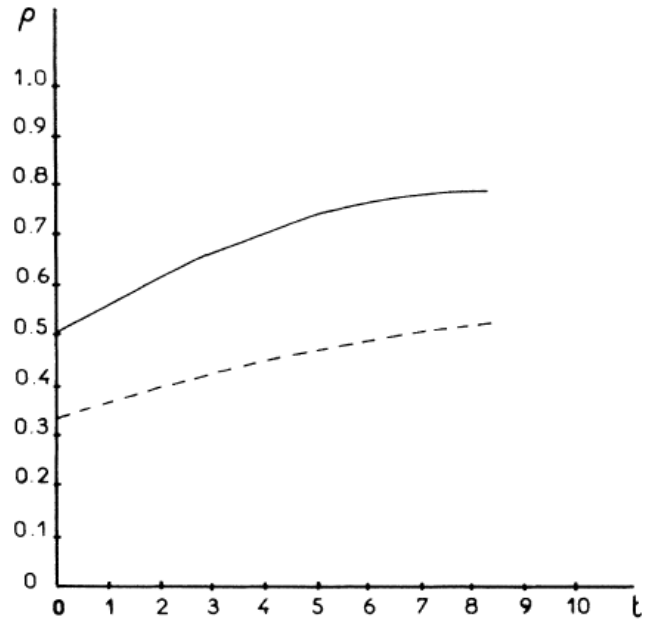

FIG. 9: Evolution of the normalized cross helicity ρ. Dashed line, random initial conditions; solid line, Orszag-Tang vortex (Pouquet et al., PRA, 1986)

In the 1980s, with evidence emerging in simulations and experiments that magnetic-invariant driven relaxation such as selective decay indeed occurs, while also the solar wind and other simulation results supporting dynamic alignment, the natural question to ask was whether both can be realized. Unfortunately the answer is immediately seen to be negative, as can easily be demonstrated. 3D MHD selective decay (or Taylor relaxation) requires minimizing $E/H_m = (E_v + E_b)/H_m$. This clearly requires that $E_v = (1/2)\langle u^2 \rangle \to 0$. Therefore one cannot also require that $\mathbf{u} = \pm \mathbf{b}$ unless both fields vanish.

How close can one get to states that compromise between the two principles? Ting et al. [144] examined this issue in 2D MHD using simulations and developed an explanation for observed final states based on minimizing energy subject to conservation of both the magnetic invariant A and the cross helicity H_c. The three dimensional version of this study was later carried out [141], using the same approach as employed by Ting et al. for 2D. The constrained minimum energy states [105, 141, 144], incorporating constraints from both selective decay and dynamic alignment principles, are determined from the variational problem

$$\delta \int \left[\left(|\boldsymbol{v}|^2 + |\boldsymbol{b}|^2 \right) - \alpha_1 \boldsymbol{v} \cdot \boldsymbol{b} - \alpha_2 \boldsymbol{a} \cdot \boldsymbol{b} \right] d^3x = 0 \qquad (12)$$

where α_i are Lagrange multipliers. The above Euler-Lagrange equation imply that in the relaxed (long-time) state equilibrium is characterized by long wavelength states that have the properties that

$$A_1 \boldsymbol{v} = A_2 \boldsymbol{b} = A_3 \boldsymbol{j} = A_4 \boldsymbol{\omega}, \qquad (13)$$

where A_1, A_2, A_3 and A_4 are constants related to the Lagrange multipliers, and $\boldsymbol{a}$ is the potential vector ($\boldsymbol{b} = \boldsymbol{\nabla} \times \boldsymbol{a}$), $\boldsymbol{j} = \nabla \times \boldsymbol{b}$ is the current density, and $\boldsymbol{\omega} = \nabla \times \boldsymbol{v}$ is the vorticity. It is noteworthy that this principle predicts the parameter space curve (as illustrated in Fig 10) towards which most numerically computed solutions eventually evolve.

The empirically demonstration that many simulation cases evolve towards the constrained minimum energy curve is rather interesting, but falls short of being a predictive theory in a few ways. First, there is no definitive way to determine precisely the position on the minimum energy curve to which a particular simulation will evolve. Second, some simulations do not evolve towards the curve, but rather some get "lost" in the middle of the space, exhausting their energy before they can evolve to a boundary. Others evolve towards the small region near the origin labeled "IV" in Fig. 10 which is characterized by vanishing magnetic field. This "hydrodynamic region" of behavior seems to be attained by turbulence with large scale, strong velocity shears. If sufficiently dominant, the strong velocity field might drive zero cross helicity fluctuations into the inertial range, thus destroying eventually the initial H_c. If the magnetic helicity is insufficient to produce a strong selective decay effect, this high shear turbulence can evolve towards a 'hydrodynamic-like" state. It is interesting that the highly Alfvénic states observed in the inner heliosphere [11] eventually evolve towards *lower* cross helicity as observed at 1AU and beyond [120]. One explanation offered for this [121] is that the shear associated with high speed-low speed stream interfaces destroys the cross helicity, as in the

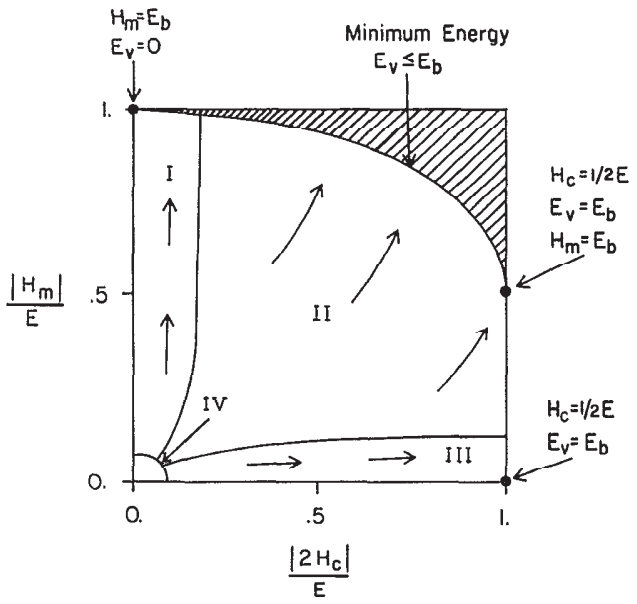

FIG. 10: Parameter space for evolution of 3D MHD spanned by axes that measure the ratios H_m/E (indicative of selective decay) and H_c/E (indicative of dynamic alignment. Evolution of a large number of simulations (a few are shown) demonstrate that most cases evolve towards the extremal curve that is analytically computed by minimizing energy subject to constancy of both H_m and H_c. From [141].

above Region IV behavior. This addresses why the solar wind apparently does not dynamically align.

It is apparent that selective decay and dynamic alignment are powerful but imperfect (or at least incomplete) principle for understanding relaxation in MHD. Efforts to describe turbulent relaxation as precisely as possible some time ago once again turned attention to the related field of 2D incompressible. Very long simulation runs in 2D periodic geometry showed that the system approached the selective decay state with regard to some metrics, but slowly [82] in part due to the tendency of isolated vortices to form [17, 86]. As vortices merge, with bursts of turbulent activity, the system ever more slowly approaches the target state of selective decay. Further quantitative study revealed [99, 100] that another principle, that of *maximum entropy* is an even better descriptor of the relaxation. In this one postulates an entropy of the form

$$S = \int \omega \log\omega \; d^2x. \tag{14}$$

and then employing variational methods it is possible to derives an equation for the maximum entropy subject to the constraint of constant energy and signed flux (see [99]). The "sinh-Poisson" equation that describes this relaxed state had derived earlier using a discrete line vortex representation [95], and the applicability of that approach to decaying viscous continuum 2D turbulence was revived following these computations (see e.g., [18, 19, 118, 119]. It is noteworthy that the correlation coefficient of the time dependent computed solution with the selective decay state in these kinds of numerical experiments eventually exceeds 90 or 95 %, but the correlation with the maximum entropy state has been measured to be as high as 0.995. By now, this experiment has been repeated numerous times.

One may of course wonder how robust this result is for various 2D hydro systems, parameters and initial condition, and in view of prior experience with relaxation in 2D MHD this would seem prudent. In fact, Huang and Driscoll [56] reported an experimental observation that selective decay is more accurate than maximum entropy as a predictor of an observed metastable state in the 2D hydro-like Penning trap electron fluid. Rodgers et al [123] reexamined this conclusion using a series of initial conditions for the electron trap experiments that varied in their initial complexity and turbulence level. (An example of one such initial condition is shown in the left panel of Fig (1). The conclusion was given that, for these particular experiments, the maximum entropy description worked at least as well as selective decay, the two descriptions being about equivalent at low levels of initial turbulence. For smaller scale more complex initial data, the maximum entropy description became progressively more favored. There is the additional element of complex plasma physics involved in these electron experiments, so the results may be considered interesting, but not conclusive in the realm of fluid theory. However it is noteworthy that in both MHD and in 2D hydro there is evidence that the distinct relaxation processes may be operative and may complete, sometimes with one only slightly favored in the evolution. Furthermore, initial data appears to be a significant factor in guiding the eventual relaxation.

The fact that a maximum entropy theory is a slightly better predictor of the final state than is selective decay in 2D hydro is noteworthy in itself and may be viewed as ample motivation to find suitable maximum entropy theories and predictions for 2D MHD and 3D MHD. However in spite of some beginnings towards this type of theory (e.g., [97]), there has not yet been to our knowledge a convincing demonstration of maximum entropy in MHD turbulence.

The above lack of clarity regarding relaxation and maximum entropy has persisted for several decades in spite of heavy mathematical methods that have been brought to bear on the subject of fluid entropies (e.g., [46]). The latter reference showed demonstrated in aa rather abstract mathematical way that solutions of the Navier Stokes equations with a single signed vorticity after long times, approach an Oseen vortex solution that is related to a maximum entropy functional such as that given above. A recent publication clarified this conclusion in a way perhaps more accessible to physicists [101]. Temporarily adopting the notation of that paper, we can consider solutions of the Navier Stokes equation in infinite 2D space without boundaries and initially a single sign of vorticity. Suppose then that the entropy Eq. (14) is maximized subject to conservation of integrated vorticity,

$$\Omega \equiv \int \omega \; d^2x = \text{const.} \tag{15}$$

and the quantity

$$\Gamma \equiv \int \frac{\omega r^2}{t} d^2x = 4\nu\Omega + \frac{1}{t}\int r^2\omega_0 \; d^2x, \tag{16}$$

which from the equation of motion, is independent of time. It is possible then to show that constrained maximum entropy solutions are of the form

$$\omega = \frac{\Omega^2}{\pi \Gamma t} \exp\left[-\Omega r^2/\Gamma t\right]. \tag{17}$$

Then as t becomes large, $\Gamma \rightarrow 4\nu\Omega$, and one finds

$$\omega \underset{t\rightarrow\infty}{\Rightarrow} \frac{\Omega}{4\pi\nu t} \exp\left[\frac{-r^2}{4\nu t}\right] \tag{18}$$

which has the form of the standard Oseen vortex solution of the Navier Stokes equation. This calculation shows that at least for this one simple case, a maximum entropy solution will emerge at long times. It may be the only case for which a unique solution to the turbulent relaxation question is known.

VII. INTERMITTENCY, DISCONTINUITIES AND MAGNETIC STRUCTURES

Simulations of magnetohydrodynamic (MHD) turbulence [14, 114] and solar wind observations [29, 53, 76, 136] each show evidence for intermittency in the form of characteristic small-scale structures. A familiar, theoretically motivated approach to characterizing intermittency is to examine the scaling of the exponents of the the higher order structure functions. Examples are shown here from MHD simulation, in Fig(11), and from solar wind observations, in Fig.(12). These scalings can be studied on their own, but, as our hydrodynamics colleagues remind us [137], the significance of these scalings is that they correspond in some way to *structure* and *enhanced dissipation.* For 2D MHD it is fairly easy to visualize this association. The highly dissipative coherent structures can be identified as current sheets that form dynamically between interacting magnetic islands [30, 78, 147]. Fig (13) demonstrates how the nonGaussian tails of the current distribution in a 2D MHD simulation correspond to strong current sheets of this type. This is less easy to demonstrate in 3D and in the solar wind.

To pursue understanding intermittency in MHD and in the solar wind, a reasonable hypothesis is that the well-known frequent appearance of structures traditionally identified as magnetic discontinuities [27, 145] (TS) are related to intermittency of turbulence. As a preliminary step, a recent simulation study [49] showed that intermittency- and discontinuity identification methods, and concluded that a substantial fraction of the observed discontinuities may be related to flux tube boundaries and intermittent structures that appear spontaneously in MHD turbulence [30, 78, 127, 146, 147].

A well-known feature of solar wind observations is, in fact, the appearance of sudden changes in the magnetic field vector, defined as directional discontinuities (DDs), which are detected throughout the heliosphere [25, 27, 102, 103, 136, 145]. These changes are often seen at time-scales of 3 to 5 minutes, although similar discontinuities are seen at smaller time scales [146]. One interpretation of magnetic discontinuities is that

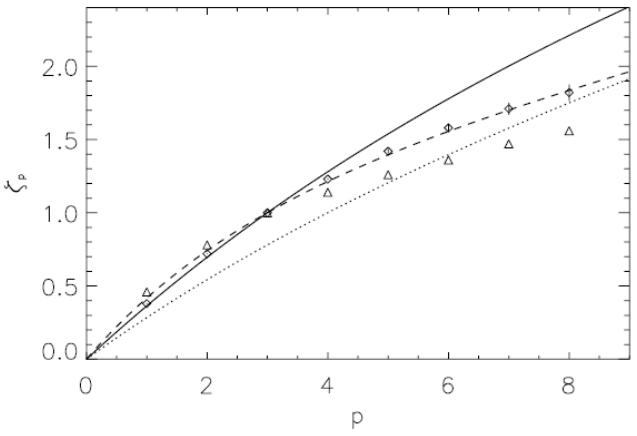

FIG. 11: Scaling exponents ζ_p for 3D MHD turbulence (diamonds) and relative exponents ζ_p/ζ_3 for 2D MHD turbulence (triangles). The continuous curve is the She-Leveque model, the dashed curve the modified model for MHD, and the dotted line the IK model. (Muller & Biskamp, PRL, 2000)

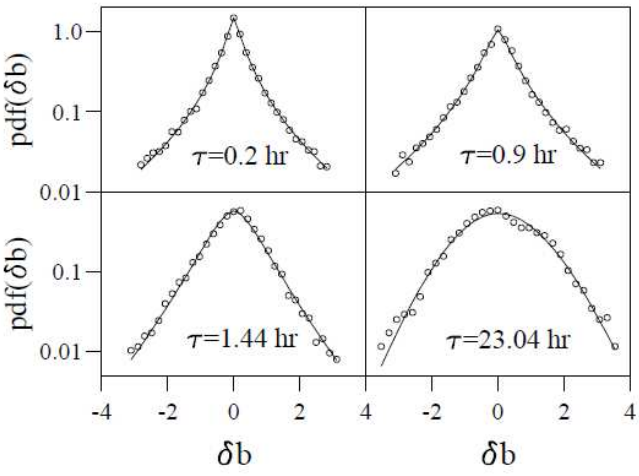

FIG. 12: The scaling behavior of the PdF for δb as calculated from the experimental data (white symbols) in the fast streams. The full lines represent the fit obtained through a model. (Sorriso-Valvo et al., GRL, 1999)

they are the walls between filamentary structures of a discontinuous solar wind plasma [25, 28]. An alternative possibility is that the observed discontinuities are the current sheets that form as a consequence of the MHD turbulent cascade [78, 148]. Recent studies on magnetic discontinuities show that their statistical properties are very similar to distributions obtained from simulations of MHD turbulence [49, 50]. This line of reasoning argues that thin current sheets are characteristic coherent structures expected in active intermittent 2D and 3D MHD turbulence [90], and which are therefore integral to the dynamical couplings across scales.

In order to establish a link between solar wind discontinuities and spatial patches of strong current sheets, here we illustrate here a comparison between solar wind datasets and direct

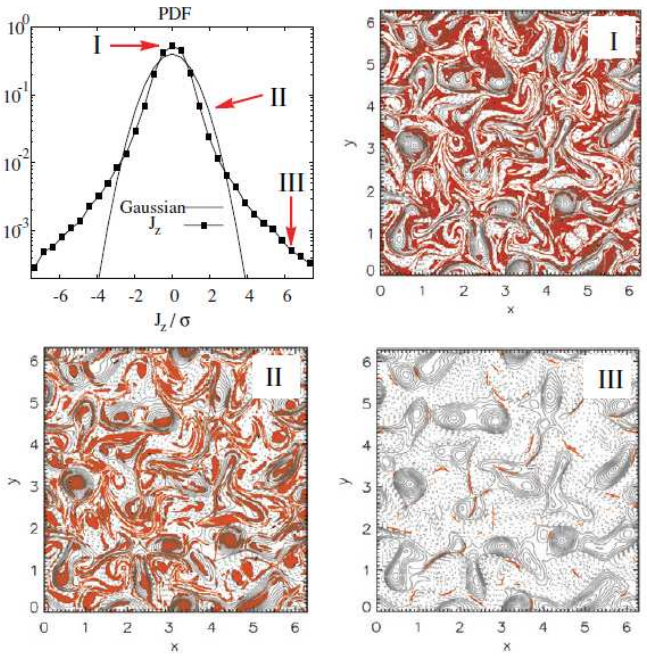

FIG. 13: PDF of the out-of-plane electric current density J_z from the 2D simulation, compared to a reference Gaussian (standard deviation σ). For each region I, II, and III, magnetic field lines (contours of constant magnetic potential A_z:$>$ 0 solid,$<$ 0 dashed) are shown; the colored (red) regions are places where the selected band (I, II, or III) contributes. (Greco et al., ApJ, 2009)

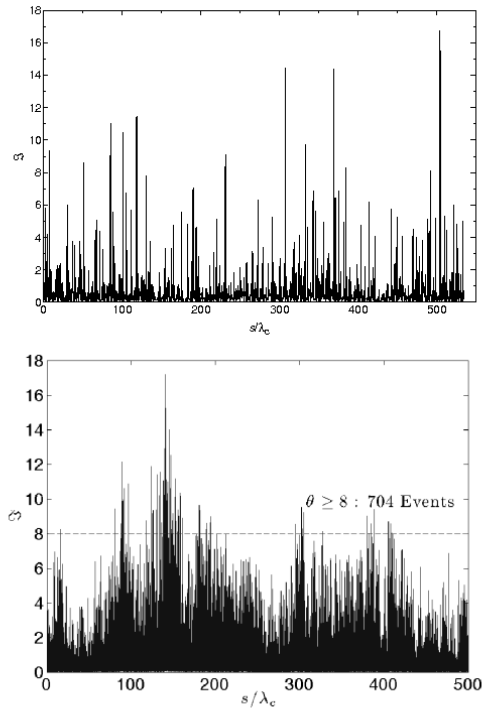

FIG. 14: Top: Spatial signal $\Im(\Delta s, \ell, s)$ (PVI) obtained from the simulation by sampling along the trajectory s in the simulation box, with $\Delta s \simeq 0.67\lambda_d$ and $\ell \simeq 535\lambda_C$. Bottom: Same quantity obtained from solar wind data, with $\Delta s = 20$ s and $\ell \simeq 500\lambda_C$.

numerical simulations of MHD. Regarding the simulations, we focus on properties of discontinuities that are recorded by magnetic field measurements at a single spacecraft in interplanetary space. We adopt a spacecraft-like sampling through the simulation domain [see Greco et al. [49]], interpolating the magnetic field data along the one-dimensional path s, we can identify discontinuities (TDs) with the following procedure:

1. First, to describe rapid changes in the magnetic field, we look at the increments

$$\Delta \boldsymbol{b}(s, \Delta s) = \boldsymbol{b}(s + \Delta s) - \boldsymbol{b}(s), \tag{19}$$

where Δs the spatial separation or lag. For this simulation we choose a small scale lag, $\Delta s \simeq 0.67\lambda_{diss}$, which is comparable to the turbulence dissipation scales (see previous sections).

2. Second, employing only the sequence of magnetic increments, we compute the normalized magnitude

$$\Im(\Delta s, \ell, s) = \frac{|\Delta \boldsymbol{b}(s, \Delta s)|}{\sqrt{\langle |\Delta \boldsymbol{b}(s, \Delta s)|^2 \rangle_\ell}}, \tag{20}$$

where $\langle \bullet \rangle_\ell = (1/\ell) \int_\ell \bullet ds$ denotes a spatial average over an interval of length ℓ, and Δs is the spatial lag in Eq. (19). The square of the above quantity has been called the *Partial Variance of Increments* (PVI) [49] and the method abbreviated as the PVI method. For the numerical analysis performed here $\ell \simeq 535\lambda_C$, where $\lambda_C = 0.18$ is the turbulence correlation length - a natural scale for computing averages.

The PVI time series, evaluated using Eqs. (19)-(20) is reported in Fig. 14. The illustration spans more than 500 correlation lengths. This spatial signal has been compared to a time signal measured by a ACE solar wind spacecraft, near 1 AU, over a period of about 20 days (lower panel of the figure). In order to facilitate the comparison, we converted the time signal to a spatial signal, using the average velocity of the flow, and then normalized to a solar wind magnetic correlation length of 1.2×10^6 km.

The PVI increment time series is bursty, suggesting the presence of sharp gradients and localized coherent structures in the magnetic field, that represent the spatial intermittency of turbulence. These events may correspond to what are qualitatively called "tangential discontinuities" and, possibly, sites of enhanced dissipation and magnetic reconnection.

Imposing a threshold θ on Eq. (20), a collection of stronger discontinuities along the path s can be identified. That is, we select portions of the trajectory in which the condition

$$\Im(\Delta s, \ell, s) > \theta \tag{21}$$

is satisfied, and we will employ this condition to identify candidate coherent structures and potential reconnection sites. To

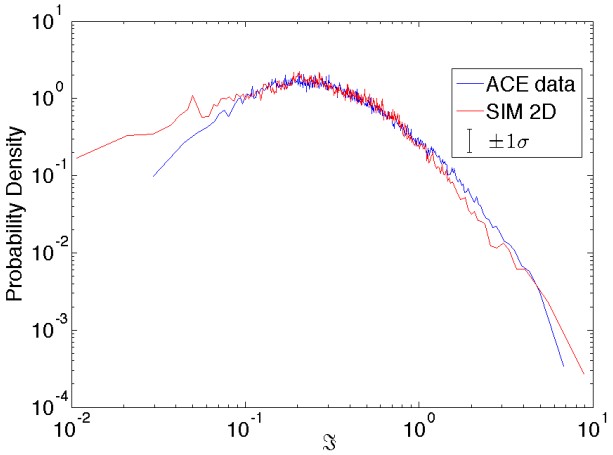

FIG. 15: Probability density function of the spatial signal $\mathfrak{A}$ (PVI) obtained from ACE measurements (blue line) and simulation (red line). The error bar $\pm\sigma$ is displayed in the legend and the value of σ is the expected fractional error in the PDF due to counting statistics.

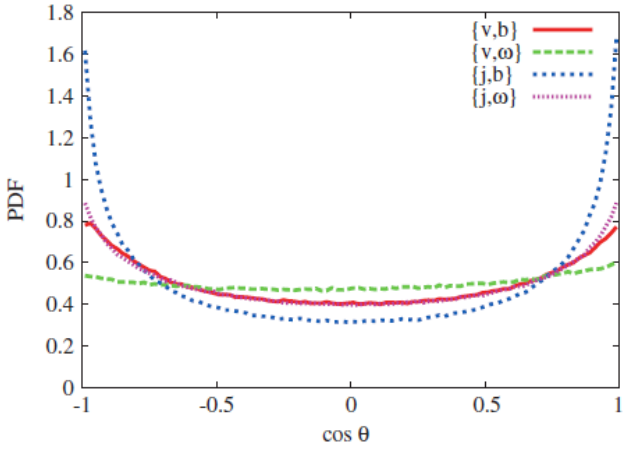

FIG. 16: PDFs of the cosine of the angle for the sets of field. (Servidio et al., PRL, 2000) The sets of fields are: $\{\boldsymbol{v}, \boldsymbol{b}\}$ (red), $\{\boldsymbol{v}, \boldsymbol{\omega}\}$ (green), $\{\boldsymbol{j}, \boldsymbol{b}\}$ (blue), $\{\boldsymbol{j}, \boldsymbol{\omega}\}$ (pink).

understand the physical meaning of the threshold θ, we recall Greco et al. [49, 50] that the probability distribution of the PVI statistic derived from a nonGaussian turbulent signal is empirically found to strongly deviate from the pdf of PVI computed from a Gaussian signal, for values of PVI greater than about 3. As PVI increases to values of 4 or more, the recorded "events" are extremely likely to be associated with coherent structures and therefore inconsistent with a signal having random phases. Thus, as θ is increased, stronger and more rare events are identified, associated with highly nonGaussian coherent structures.

Finally, in Fig. 15, we show the probability distribution functions of the PVI signal for both the observational and simulation data. The comparison tells us that there is a great similarity within the errors [107].

VIII. LOCAL RELAXATION AND NONGAUSSIANITY

The two central features of MHD turbulence discussed in the last two sections are generally studied independently: intermittency of inertial range fluctuations, and MHD relaxation processes. The first manifests trough the appearance of high kurtosis of vorticity and current, multi-fractal scaling of moments, and inhomogeneous dissipation of energy (in space). The second is characterized by distinctive states such as Taylor relaxation, selective decay, global dynamic alignment, and helical dynamo action [78, 88, 105, 141, 142, 144]. As described above, relaxation has most often viewed as a consequence of multiple global ideal conservation principles, characterized by dynamical times much longer than the characteristic times of intermittency.

Recently [127], it has been demonstrated that undriven MHD turbulence spontaneously generates coherent spatial correlations of several types, associated with local Beltrami fields, local Alfvénic correlations, i.e., directional alignment of velocity and magnetic fields, local force free states, and anti-alignment of magnetic and fluid acceleration components. These correlations suppress nonlinearity to levels lower than what is obtained from Gaussian fields, and occur in spatial patches. These are not true quasi-equilibria, as the nonlinearity is only very rarely fully suppressed, but the systematic occurrence of these correlations indicates that the turbulence adjusts to the presence of large forces through a rapid dynamical response to reduce these stresses. These rapid relaxation processes are necessarily local, simultaneously occurring in various locations without regard to global compatibility other than the global conservation laws. Intuitively, this picture gives rise to a cellularization of the turbulence, which is in fact observed in simulations [85, 127] and in the solar wind [108].

To demonstrate the rapid local relaxation of MHD turbulence, we illustrate the distributions (PDFs) of the angle [66, 106]

$$\cos\theta = \frac{\mathbf{f}\cdot\mathbf{g}}{|\mathbf{f}||\mathbf{g}|} \tag{22}$$

where $\{\mathbf{f}, \mathbf{g}\}$ represents one of $\{\boldsymbol{v}, \boldsymbol{b}\}$, $\{\boldsymbol{v}, \boldsymbol{\omega}\}$, $\{\boldsymbol{j}, \boldsymbol{b}\}$ and $\{\boldsymbol{j}, \boldsymbol{\omega}\}$. In Fig. 16 these four PDFs are shown. The initial Gaussian distribution with null (net) helicities corresponds to imposing a flat initial distribution of Eq. (22). Quickly, as the nonlinearity develops, strong alignments appear. These aligned (anti-aligned) fields correspond to a Beltramization of the magnetofluid, similar to the Navier-Stokes (NS) case. Even though global helicities remain small, the magnetofluid locally self-organizes into patches which contain several types of correlations.

Since the conclusions bear a close resemblance to the properties of 3D MHD global relaxation, it is tempting to extend the original interpretations. Global long time relaxation gives rise to the same Beltrami properties as suggested in Fig (16), for both velocity $\boldsymbol{v}$ and magnetic $\boldsymbol{b}$ fields. These emerge from variational principles [78, 96, 144] in which minimum energy states [105, 141, 144] are solutions to Eq. (12). The asso-

ciated Euler-Lagrange equations imply that the relaxed states are described by: $\boldsymbol{v} \propto \boldsymbol{b} \propto \boldsymbol{j} \propto \boldsymbol{\omega}$, where $\boldsymbol{a}$ the potential vector ($\boldsymbol{b} = \boldsymbol{\nabla} \times \boldsymbol{a}$), $\boldsymbol{j} = \nabla \times \boldsymbol{b}$ is the current density, and $\boldsymbol{\omega} = \nabla \times \boldsymbol{v}$ is the vorticity. In global relaxation, these conditions are applied to the entire system and at large times, with the coefficients of proportionality implied in Eq. (13) take to be uniform constants. However the observation of local patches of enhanced Beltrami, force free and Alfvénic correlations at short times suggests another interpretation in which the coefficients of proportionality defining the generalized Beltrami states are viewed as piecewise constant and time varying. It remains for further work to show if this description can adequately account for the cellular structure of MHD turbulence, in which patches of correlation are bounded by near-discontinuous slowly evolving coherent structures that separate the relaxed regions.

There are numerous quantitative implication of the above picture of rapid relaxation, only some of which have been examined so far. One consequence of the increased probability of occurrence of the Beltrami correlations ($\cos\theta = \pm 1$) is the emergence of regions in which the nonlinear term has become suppressed and the energy cascade has become inhibited [59]. From a simple look at the MHD equations, the alignment observed in Fig. 16 suggests that the strength of the nonlinear term is "suppressed" [127]. Indeed, quantitative examination of simulations data has shown that the turbulent accelerations ($|\frac{\partial \boldsymbol{v}}{\partial t}|$, $|\frac{\partial \boldsymbol{b}}{\partial t}|$) are much weaker that if they were computed with a Gaussian (random) field [127].

While the rapid-alignment processes occur, suppressing the strength of the nonlinear terms, it was also shown that enhancement of the kurtosis occurs, thus supporting the interpretation as the development of "cells". The kurtosis is an elementary measure of the degree of the intermittency of the system. Therefore if the suppression is driven by nonlinear relaxation, then one would expect to see signatures of coherent structure formation even in ideal flows. Indeed it was suggested years ago [42] that current sheets form exponentially fast in ideal MHD. Recently analysis of both dissipative and ideal 2D MHD simulations demonstrated that spectral transfer, beginning from band limited Gaussian initial conditions, gives rise to high kurtosis excitations at the higher wavenumbers.[150], even at very early times.

The overall picture, in which it may be possible to understand the close linkages between cascade and intermittency, between rapid local relaxation and suppression of nonlinearity, between coherent structures and cellular boundaries, and ultimately between slow global relaxation and fast local relaxation, remain far from complete. The connections reviewed above have been established in both 2D nd 3D MHD studies, bu the picture in 3D is of course less clear, due to both to physical complexity and numerical limitations. Much more work will be needed to complete this picture, and to establish a firmer analytical understanding beyond the sketchy suggestions implied above.

It does appear however that a general view is emerging that the nonlinear dynamics of decaying 3D incompressible MHD leads spontaneously to several rapid, local relaxation processes, favoring states having strong alignments or anti-alignments different fields, namely those that suppress the strength of nonlinearities.. The production of spatial patches of these correlations requires that the statistical distribution of velocity and magnetic field become nonGaussian, as can be seen by formulating the correlations of (at least) fourth order, such as $\langle(\mathbf{v}\cdot\mathbf{b})^2\rangle$ that must grow to form Alfvénic patches Our conclusion is that this multifaceted rapid relaxation is intimately related to the formation of spatial intermittent structures. A simple real space picture emerges: when patches of suppression of nonlinearity are formed, the fourth order statistics become nonGaussian, as the gradients become concentrated along boundaries of the patches. For example, two regions can become approximately force free, but the boundary between them will not be force free [22]. This would concentrate nonlinear activity near cellular boundaries of turbulence. Magnetic reconnection is one example of the type activity that can occur at these boundaries [129].

IX. THIRD ORDER LAW IN MHD

A well known Kolmogorov–Yaglom ("4/5") law relates the third-order structure function to the energy dissipation rate [40, 60, 94]. Usually it is stated with the assumptions of isotropy, homogeneity, and time stationarity of the statistics of velocity increments $\delta\boldsymbol{u} = \boldsymbol{u}(\boldsymbol{x}+\boldsymbol{r}) - \boldsymbol{u}(\boldsymbol{x})$ [velocity $\boldsymbol{u}$, spatial positions $\boldsymbol{x}+\boldsymbol{r}$ and $\boldsymbol{x}$]. It also apparently requires adoption of the von Kármán hypothesis [58] that the rate of energy dissipation ϵ approaches a constant nonzero value as Reynolds number tends to infinity. Without the need for assuming isotropy, one finds

$$\frac{\partial}{\partial r_i}\left\langle \delta u_i \left|\delta\boldsymbol{u}\right|^2 \right\rangle = -4\epsilon, \tag{23}$$

where $\langle\cdots\rangle$ indicates an ensemble average and a sum on repeated indices is implied. If isotropy is further assumed then,

$$\left\langle \delta u_L \left|\delta\boldsymbol{u}\right|^2 \right\rangle = -\frac{4}{d}\epsilon\left|\boldsymbol{r}\right|, \tag{24}$$

where d is the number of spatial dimensions and $\delta u_L = \hat{\boldsymbol{r}}\cdot\delta\boldsymbol{u}$ is the increment component measured in the direction of the unit vector $\hat{\boldsymbol{r}}$ parallel to the relative separation $\boldsymbol{r}$.

Extension of the third-order law to the case of incompressible MHD was reported by Politano and Pouquet [113], who remained close to the approximations made in the hydrodynamic case. Without assuming isotropy, they found

$$\frac{\partial}{\partial r_i}\left\langle \delta z_i^{\mp}\left|\delta\boldsymbol{z}^{\pm}\right|^2 \right\rangle = -4\epsilon^{\pm}, \tag{25}$$

which, after adoption of isotropy, reduces to,

$$\left\langle \delta z_L^{\mp}\left|\delta\boldsymbol{z}^{\pm}\right|^2 \right\rangle = -\frac{4}{d}\epsilon^{\pm} r, \tag{26}$$

where $\delta\boldsymbol{z}^{\pm} = \boldsymbol{z}^{\pm}(\boldsymbol{x}+\boldsymbol{r}) - \boldsymbol{z}^{\pm}(\boldsymbol{x})$ are the increments of the Elsässer variables and $\delta z_L^{\pm} = \hat{\boldsymbol{r}}\cdot\delta\boldsymbol{z}^{\pm}$. The constants $\epsilon^{\pm}$ are the mean energy dissipation rates of the corresponding variables

$\boldsymbol{z}^{\pm} = \boldsymbol{u} \pm \boldsymbol{b}$, where $\boldsymbol{b}$ is the magnetic field fluctuation in Alfvén speed units.

There has been a flurry of activity in the past few years, geared towards measurement of the cascade rate in the solar wind using various forms of the isotropic third order law [74, 75, 135, 138], including the anisotropic form. [109] Many of these estimates arrive at heating rates around 10^4 JKg^{-1}s^{-1}, which agrees well with estimates from temperature gradients [146]. (See also Coleman (1968) [33].)

X. EXTENSION TO KRSH AND INTERMITTENCY OF DISSIPATION

The Kolmogorov Refined Similarity Hypothesis (KRSH) [61] is the unproven but extraordinarily useful theoretical construct that connects the probability distributions of inertial range increments and averages of the dissipation function [104, 137]. The extension to MHD is not completely straightforward, for the usual reasons that there is more than one cascaded field, and ambiguities arise. For a useful starting place, see [87]. It is noteworthy that the KRSH might be formally viewed as the motivation for scaling studies of higher order structure functions, yet, as described above, this activity has proceeded [14, 53, 76, 114, 136], in spite of the absence of a clear statement of the correct form of the hypothesis. (This may be an oxymoron of sorts, since it is in the end KRSH is a working hypothesis.)

Apart from complications associated with MHD Theory, application of KRSH extensions to low density solar wind and astrophysical plasmas must confront another great problem – we do not know the correct functional form of the dissipation function, or even the complete roster of appropriate physical process to include in it. The problem of examining possible dissipation processes in the solar wind and interstellar medium is a very active one at present, and a complete review would be well outside the present scope. For a few starting points, see [2, 3, 68–70, 126, 134]. A fuller understanding of this problem is a great challenge for the coming years.

As a final remark on this point we note that for a low density space plasma one might expect to find relationships of the form (schematically)

$$\frac{\delta Z_s^3}{s} \sim \epsilon_s \rightarrow T_s \tag{27}$$

where δZ_s is a measure of the (possibly mixed) magnitude of vector increments at separation s, ϵ_s is the average of the dissipation function over scale s, and T_s is a measure of the similarly averaged temperature, or perhaps the local temperature excess. The first relationship in Eq (27) is akin to the KRSH, although the precise form of the increment might be a fruitful topic of conversation (see [87]). The second relationship is even less clear, although intuitively it seems that if one deposits a large amount of heat locally, the temperature very well might increase. The first relationship cannot be examined in the solar wind because we do not know ϵ. The second relationship cannot be examined in most simulations because they are incompressible, and in any case we do not know the correct form of the heat conduction for a plasma such as the solar wind. But what we can do is assume the second relationship and then compare increments to temperature averages in the solar wind. This was done recently by Osman et al (2011) [107]. The approach was to employ the PVI statistic discussed above in an earlier section to find locations of near-discontinuous magnetic structure. The higher values of PVI indicate more rare and stronger discontinuities. Then the proton temperature (and other diagnostics) were conditionally sampled for increasing PVI. One such result is reproduced here in Fig (17). It is readily apparent that the samples with large PVI are hotter on average and have hotter tails. This is completely consistent with the idea that the dissipation function, whatever it is in the solar wind, is more active within and near the coherent structures. Evidently the solar wind plasma, even though it is not hydrodynamics nor even precisely an MHD medium, shares with classical turbulence the ideas that the dissipative structures are localized, providing a meaning to the ideas of intermittency for this plasma that is similar to what Kolmogorov's ideas mean for hydrodynamics.

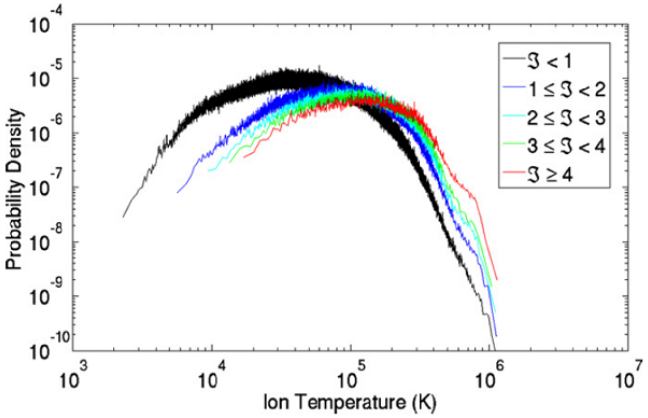

FIG. 17: PDFs of the ion temperature, where each PDF corresponds to a different range of PVI values. As the PVI values increase, the probability density decreases at lower temperatures and increases at higher temperatures. Also, the mean ion temperature increases with increasing PVI. The corresponding PDFs for electron heat flux magnitude, electron temperature, and local dissipation behave in a similar manner. (Osman et al., ApJ, 2011)

XI. CONCLUSIONS AND OMISSIONS

MHD turbulence and its applications to real physical systems remains a fascinating, complex and rapidly developing field of physics. Naturally many of its features remains close to their hydrodynamic antecedents, but numerous new complications arise. Here we aimed to provide a quick sampling of some MHD results for homogeneous plasmas, for related systems in 2D hydro and electron plasmas, and for a major field of application in the solar wind. The subject is big enough that a complete review of even these special topics has not been possible, and we apologize for what have doubt-

less been numerous and egregious oversights on the discussion and references. Furthermore we made essentially no attempt to cover very important fields such as laboratory plasmas, astrophysics, magnetic reconnection, planetary, stellar and laboratory dynamo theory, MHD power generation and otherd industrial applications, as well as deeper connections with plasma physics through multispecies fluid models and other variants of the MHD plasma. The omission of discussion of relaxation in laboratory reversed field pinch, spheromak and tokamak plasmas is particularly egregious due to the close relationship those studies have to those that are included here. For excellent reviews and introductory material in these areas, see [22, 23, 54, 143]. Another major deficiency here is the lack of discussion of closures [48, 116]. An interesting and high-powered example is the two-scale direct interaction approximation that has been applied to development of tractable MHD closures (e.g., [155]. These indeed have the potential to make progress in problems of current interest [154]; however, as with other interesting subjects, there has not been an opportunity to delve into that interesting subject here.

We hope that, within the limited context of the sample provided here, there may be adequate connections afforded by the references for an interested reader to get a foot hold in a few interesting problems relating to turbulence in magnetized fluids, and in the physics of the solar wind.

Acknowledgments

This research has been supported by the NSF SHINE program ATM-0752135, the Solar Terrestrial program AGS-1063439, and by NASA through the MMS mission NNX08AT76G, the Solar Probe Mission (ISIS subcontract, and the Heliophysics Theory program. WHM is grateful for the hospitality of the University of Calabria, the assistance of Lorenzo Servidio, and the support for collaborators from the EU TURBOPLASMA program.

[1] A. Alexakis, P. D. Mininni, and A. Pouquet, "Shell-to-shell energy transfer in magnetohydrodynamics. I. Steady state turbulence.", Phys. Rev. E. **72**, 046301 (2005).

[2] Alexandrova, O., Saur, J., Lacombe, C., et al. 2009, Physical Review Letters, 103, 165003

[3] S. D. Bale, et al., "Magnetic fluctuation power near proton temperature anisotropy instability thresholds in the solar wind." Phys. Rev. Lett. **103**, 211101 (2009).

[4] A. Balogh, et al., "The Cluster magnetic field investigation: overview of in-flight performance and initial results", Ann. Geophys., **19**, 1207 (2001).

[5] A. Barnes, "Collisionless heating of the solar-wind plasma, 1. Theory of the heating of collisionless plasma by hydromagnetic waves." *Astrophys. J.*, **154**, 751 (1968).

[6] Aaron Barnes. "Hydromagnetic waves and turbulence in the solar wind." In E. N. Parker, C. F. Kennel, and L. J. Lanzerotti, editors, *Solar System Plasma Physics, vol. I*, page 251, Amsterdam, North-Holland, 1979.

[7] G. K. Batchelor, "Computation of the energy spectrum in homogeneous two-dimensional turbulence", Phys. Fluids, **12**, II-233 (1968).

[8] B. Bavassano, M. Dobrowolny, F. Mariani, and N. F. Ness. "Radial evolution of power spectra of interplanetary Alfvénic turbulence." *J. Geophys. Res.*, **87**, 3617 (1982).

[9] B. Bavassano, M. Dobrowolny, G. Fanfoni, F. Mariani, and N. F. Ness, "Statistical properties of MHD fluctuations associated with high-speed streams from Helios-2 observations." *Solar Phys.*, **78**, 373 (1982).

[10] B. Bavassano and E. J. Smith, "Radial Variation of Interplanetary Alfvénic Fluctuations: Pioneer 10 and 11 Observations Between 1 and 5 AU", J. Geophys. Res. **91**, 1706 (1986).

[11] J. W. Belcher and L. Davis Jr. "Large-amplitude Alfvén waves in the interplanetary medium, 2." *J. Geophys. Res.*, **76**, 3534 (1971).

[12] J. W. Bieber, W. H. Matthaeus, C. W. Smith, W. Wanner, M. Kallenrode, and G. Wibberenz. "Proton and electron mean free paths: The Palmer consensus revisited." *Astrophys. J.*, **420**, 294 (1994).

[13] J. W. Bieber, W. Wanner, and W. H. Matthaeus. "Dominant two-dimensional solar wind turbulence with implications for cosmic ray transport." *J. Geophys. Res.*, **101**, 2511 (1996).

[14] D. Biskamp and W.-C. Muller, "Scaling properties of three-dimensional isotropic magnetohydrodynamic turbulence." Phys. Plasmas, **7**, 4889 (2000).

[15] D. Biskamp, Magnetohydrodynamic Turbulence, Cambridge University Press, Cambridge, 2003.

[16] A. Bondeson, G. Marklin, Z. G. An, H. H. Chen, Y. C. Lee, and C. S. Liu, "Tilting instability of a cylindrical spheromak ", **24**, 1682 (1981).

[17] M. Brachet, M. Meneguzzi, H. Politano, and P.-L. Sulem, "The dynamics of freely decaying two-dimensional turbulence." J. Fluid Mech. **194**, 333 (1988).

[18] H. Brands, J. Stulemeyer, R. A. Pasmanter, and T. J. Schep. "A mean field prediction of the asymptotic state of decaying 2D turbulence." *Phys. Fluids*, **9**, 2815 (1997).

[19] H. Brands, P. H. Chavanis, R. Pasmanter, and J. Sommeria. "Maximum entropy verses minimum enstrophy vortices." *Phys. Plasmas*, **11**, 3465 (1999).

[20] B. Breech, W. H. Matthaeus, J. Minnie, J. W. Bieber, S. Oughton, C. W. Smith, and P. A. Isenberg. "Turbulence transport throughout the heliosphere." *J. Geophys. Res.*, **113**, A08105 (2008).

[21] B. Breech, W. H. Matthaeus, S. R. Cranmer, J. C. Kasper, and S. Oughton, "Electron and proton heating by solar wind turbulence", J. Greophys. Res. **114**, A09103 (2009).

[22] M. R. Brown, "Experimental Evidence of Rapid Relaxation to Large Scale Structures in Turbulent Fluids: Selective Decay and Maximal Entropy."J. Plasma Phys. **57**, 203 (1996).

[23] M. R. Brown, "Experimental studies of magnetic reconnection", Phys. Plasmas, **6**, 1717 (1999).

[24] R. Bruno, B. Bavassano, and U. Villante, "Evidence for long period Alfvén waves in the inner solar system." J. Geophys. Res. **90**, 4373 (1985).

[25] R. Bruno, V. Carbone, P. Veltri, E. Pietropaolo, and B. Bavassano, "Identifying intermittency events in the solar wind." Planet. Space Sci., **49**, 1201 (2001).

[26] Roberto Bruno and Vincenzo Carbone, "The Solar Wind as a Turbulence Laboratory", Living Rev. Solar Phys. 2, (2005), 4.

URL: http://www.livingreviews.org/lrsp-2005-4
[27] L. F. Burlaga, "Micro-Scale Structures in the Interplanetary Medium." Solar Phys., **4**, 67 (1968).
[28] L. F. Burlaga, "Directional Discontinuities in the Interplanetary Magnetic Field", Solar Phys., **7**, 54 (1969).
[29] L. F. Burlaga, "Intermittent turbulence in the solar wind." J. Geophys. Res. **96**, 5847 (1991).
[30] V. Carbone, P. Veltri, and A. Mangeney, "Coherent structure formation and magnetic field line reconnection in magnetohydrodynamic turbulence." Phys. Fluids A, **2**, 1487 (1990).
[31] S. Chandrasekhar and L. Woltjer, "On force-free magnetic fields", Proc. National Acad. Sci. USA, **44**, 285 (1958).
[32] S. Chen, and R. H. Kraichnan, "Inhibition of turbulent cascade by sweep", J. Plasma Phys. **57**, 187 (1997).
[33] P. J. Coleman, "Turbulence, Viscosity, and Dissipation in the Solar-Wind Plasma", Astrophys. J. **153**, 371 (1968).
[34] S. R. Cranmer, "Coronal Holes," Living Rev. Solar Phys. **6** (2009).
[35] S. R. Cranmer, W. H. Matthaeus, B. A. Breech, and J. C. Kasper, "Empirical constraints on proton and electron heating in the fast solar wind." Astrophys. J., **702**, 1604 (2009).
[36] P. Dmitruk and W. H. Matthaeus. "Low-frequency 1/f fluctuations in hydrodynamic and magnetohydrodynamic turbulence." *Phys. Rev. E*, **76**, 036305 (2007).
[37] P. Dmitruk, P. D. Mininni, A. Pouquet, S. Servidio, and W. H. Matthaeus, "Emergence of very long time fluctuations and 1/f noise in ideal flows", Phys. Rev. E. **83**, 066318 (2011).
[38] M. Dobrowolny, A. Mangeney, and P. Veltri. "Fully developed anisotropic hydromagnetic turbulence in interplanetary space." *Phys. Rev. Lett.*, **45**, 144 (1980).
[39] C. F. Driscoll and K. S. Fine. "Experiments on vortex dynamics in pure electron plasmas." *Physics of Fluids B*, **2**, 1359 (1990).
[40] U. Frisch, Turbulence, Cambridge University Press, Cambridge, 1995.
[41] Uriel Frisch, A. Pouquet, J. Léorat, and A. Mazure. "Possibility of an inverse cascade of magnetic helicity in magnetohydrodynamic turbulence." *J. Fluid Mech.*, **68**, 769, (1975).
[42] U.Frisch, A.Pouquet, P.-L.Sulem, and M.Meneguzzi, "The dynamics of two-dimensional ideal MHD." J.Mech.Theor.Appl, **2**, 191 (1983).
[43] D. Fyfe and D. Montgomery. "High beta turbulence in two-dimensional magnetohydrodynamics." *J. Plasma Phys.*, **16**, 181–191, (1976).
[44] D. Fyfe, G. Joyce, and D. Montgomery. "Magnetic dynamo action in two-dimensional turbulent magnetohydrodynamics." *J. Plasma Phys.*, **17**, 317, (1977).
[45] D. Fyfe, D. Montgomery, and G. Joyce. "Dissipative, forced turbulence in two-dimensional magnetohydrodynamics." *J. Plasma Phys.*, **17**, 369, (1977).
[46] T. Gallay and C. E. Wayne, "Global stability of vortex solutions of the twodimensional Navier-Stokes equation." Comm. Math. Phys. **255**, 97 (2005).
[47] P. Goldreich and S. Sridhar. "Toward a theory of interstellar turbulence: II. Strong Alfvénic turbulence." *Astrophys. J.*, **438**, 763 (1995).
[48] R. Grappin, U. Frisch, J. Léorat, and A. Pouquet. "Alfvénic fluctuations as asymptotic states of MHD turbulence." *Astron. Astrophys.*, **105**, 6 (1982).
[49] A. Greco, P. Chuychai, W. H. Matthaeus, S. Servidio, and P. Dmitruk, "Intermittent MHD structures and classical discontinuities", Geophys. Res. Lett., **35**, L19111 (2008).
[50] A. Greco, W. H. Matthaeus, S. Servidio, P. Chuychai, and P. Dmitruk, "Statistical Analysis of Discontinuities in Solar Wind ACE Data and Comparison with Intermittent MHD Turbulence", Astrophys. J., **691**, L111 (2009).
[51] K. Hamilton, C. W. Smith, B. J. Vasquez, and R. J. Leamon. "Anisotropies and helicities in the solar wind inertial and dissipation ranges at 1 AU." *J. Geophys. Res.*, **113**, A01106 (2008).
[52] J. V. Hollweg. "Alfvén waves in the solar wind: Wave pressure, Poynting flux, and angular momentum." *J. Geophys. Res.*, **78**, 3643 (1973).
[53] T. A. Horbury, A. Balogh, R. J. Forsyth, and E. J. Smith, "Ulysses observations of intermittent heliospheric turbulence." Adv. Space Phys. **19**, 847 (1997).
[54] W. Horton, Drift waves and transport, Rev. Mod. Phys., 71, 735 (1999).
[55] M. Hossain, P. C. Gray, D. H. Pontius Jr., W. H. Matthaeus, and S. Oughton, "Phenomenology for the decay of energy-containing eddies in homogeneous MHD turbulence." *Phys. Fluids*, **7**, 2886 (1995).
[56] X.-P. Huang and C. F. Driscoll, "Relaxation of 2D turbulence to a metaequilibrium near the minimum enstrophy state." *Phys. Rev. Lett.*, **72**, 2187 (1994).
[57] P. S. Iroshnikov, "Turbulence of a conducting fluid in a strong magnetic field." Sov. Astron. **7**, 566 (1964).
[58] T. de Kármán and L. Howarth. "On the statistical theory of isotropic turbulence." *Proc. Roy. Soc. London Ser. A*, **164**, 192 (1938).
[59] R.M. Kerr, "Histograms of helicity and strain in numerical turbulence." Phys. Rev. Lett. **59**, 783 (1987).
[60] A. N.Kolmogorov, "Dissipation of energy in the locally isotropic turbulence." C.R. Acad. Sci. U.R.S.S., **32**, 16 (1941), [Reprinted in Proc. R. Soc. London, Ser. A **434**, 15 (1991)].
[61] A. N. Kolmogorov, "A refinement of previous hypotheses concerning the local structure of turbulence in a viscous incompressible fluid at high Reynolds number." *J. Fluid Mech.*, **12**, 82 (1962).
[62] R. H. Kraichnan, "Helical turbulence and absolute equilibrium", J. Fluid Mech. **59**, 745 (1973).
[63] R. H. Kraichnan. "Inertial-range spectrum of hydromagnetic turbulence." *Phys. Fluids*, **8**, 1385 (1965).
[64] R. H. Kraichnan, "Inertial ranges in two-dimensional turbulence." *Phys. Fluids*, **10**, 1417 (1967).
[65] R. H. Kraichnan. "Statistical dynamics of two-dimensional flow." *J. Fluid Mech.*, **67**, 155 (1975).
[66] R.H. Kraichnan and R. Panda, "Depression of nonlinearity in decaying isotropic turbulence." Phys. Fluids **31**, 2395 (1988).
[67] J. M. Kriesel and C. F. Driscoll, "Measurements of viscosity in pure-electron plasmas", Phys. Rev. Lett. **87**, 135003 (2001).
[68] R. J. Leamon, C. W. Smith, N. F. Ness, W. H. Matthaeus, and H. K. Wong, "Observational constraints on the dynamics of the interplanetary magnetic field dissipation range", J. Geophys. Res. **103**, 4775 (1998).
[69] R. J. Leamon, C. W. Smith, N. F. Ness, and H. K. Wong. "Dissipation range dynamics: Kinetic Alfvén waves and the importance of β_e." *J. Geophys. Res.*, **104**, 22331 (1999).
[70] R. J. Leamon, W. H. Matthaeus, C. W. Smith, G. P. Zank, D. J. Mullan, and S. Oughton. "MHD-driven kinetic dissipation in the solar wind and corona." *Astrophys. J.*, **537**, 1054 (2000).
[71] T. D. Lee, "On some Statistical properties of hydrodynamical and magneto-hydrodynamical fields." Q. Appl. Maths, **10**, 69 (1952).
[72] E. Lee, M. E. Brachet, A. Pouquet, P. D. Mininni, and D. Rosenberg, "Lack of universality in decaying magnetohydrodynamic turbulence", Phys. Rev. E, **81**, 016318 (2010).
[73] M. Lesieur. *Turbulence in Fluids*. Kluwer, Dordrecht, The Netherlands, 2nd edition, 1990.

[74] B. T. MacBride, M. A. Forman, and C. W. Smith, "Turbulence and third moment of fluctuations: Kolmogorov's 4/5 law and its MHD analogues in the solar wind." in Proc. Solar Wind 11: Connecting Sun and Heliosphere, ed. B. Fleck & T.H.Zurbuchen (ESASP-592; TheNetherlands: EuropeanSpaceAgency), 613 (2005).

[75] B. T. MacBride, C. W. Smith, and M. A. Forman. "The turbulent cascade at 1 AU: Energy transfer and the third-order scaling for MHD. *Astrophys. J.*, **679**, 1644 (2008).

[76] E. Marsch, and C.-Y. Tu, "Non-Gaussian probability distributions of solar wind fluctuations." Ann. Geophys. **12**, 1127 (1994).

[77] Eckart Marsch, "Kinetic Physics of the Solar Corona and Solar Wind", Living Rev. Solar Phys. 3, (2006), 1. URL (cited on ¡date¿): http://www.livingreviews.org/lrsp-2006-1 .

[78] W. H. Matthaeus and D. Montgomery. "Selective decay hypothesis at high mechanical and magnetic Reynolds numbers." *Annals of the New York Academy of Sciences*, **357**, 203 (1980).

[79] W. H. Matthaeus and M. L. Goldstein, "Measurement of the rugged invariants of magnetohydrodynamic turbulence." J. Geophys. Res. **87**, 6011 (1982).

[80] W. H. Matthaeus and D. Montgomery. "Dynamic alignment and selective decay in MHD." In C. W. Jr Horton and L. E. Reichl, editors, *Statistical Physics and Chaos in Fusion Plasmas*, pages 285–291, New York, 1984. Wiley.

[81] W. H. Matthaeus, M. L. Goldstein, and D. A. Roberts, "Evidence for the presence of quasi-two-dimensional nearly incompressible fluctuations in the solar wind." J. Geophys. Res. **95**, 20673 (1990).

[82] W. H. Matthaeus, W. T. Stribling, D. Martínez, S. Oughton, and D. Montgomery, "Selective decay and coherent vortices in two-dimensional incompressible turbulence." *Phys. Rev. Lett.*, **66**, 2731 (1991).

[83] W. H. Matthaeus, S. Dasso, J. M. Weygand, L. J. Milano, C. W. Smith, and M. G. Kivelson. "Spatial Correlation of Solar-Wind Turbulence from Two-Point Measurements". *Phys. Rev. Lett.*, **95**, 231101 (2005).

[84] W. H. Matthaeus, B. Breech, P. Dmitruk, A. Bemporad, G. Poletto, M. Velli, and M. Romoli. "Density and Magnetic Field Signatures of Interplanetary 1/f Noise." *Astrophys. J.*, **657**, L121 (2007).

[85] W. H. Matthaeus, A. Pouquet, P. D. Mininni, P. Dmitruk, and B. Breech. "Rapid Alignment of Velocity and Magnetic Field in Magnetohydrodynamic Turbulence." *Physical Review Letters*, **100**, 085003 (2008).

[86] J. C. McWilliams, "Emergence of isolated coherent vortices in turbulent flow." J. Fluid Mech. **146**, 21 (1984).

[87] J. A. Merrifield, W.-C. Müller, S. C. Chapman, and R. O. Dendy. "The scaling properties of dissipation in incompressible isotropic three-dimensional magnetohydrodynamic turbulence." *Phys. Plasmas*, **12**, 022301 (2005).

[88] P.D. Mininni, D.O. Gómez, and S.M. Mahajan, "Dynamo Action in Hall Magnetohydrodynamics." Astrophys. J. **567**, L81 (2002).

[89] P. D. Mininni, D. Montgomery, and A. Pouquet, "A numerical study of the alpha model for two-dimensional magnetohydrodynamic turbulent flows ." Phys. Fluids, **17**, 035112 (2005).

[90] P. D. Mininni, and A. Pouquet, "Finite dissipation and intermittency in magnetohydrodynamics", Phys. Rev. E, **80**, 025401 (2009).

[91] P. D. Mininni, P. Dmitruk, W. H. Matthaeus, and A. Pouquet, "Large-scale behavior and statistical equilibria in rotating flows", Phys. Rev. E. **83**, 016309 (2011).

[92] T. B. Mitchell, X. J. Wang, and L. F. Rossi. Stability of Elliptical Electron Vortices. In M. Drewsen, U. Uggerhoj, & H. Knudsen, editor, *Non-Neutral Plasma Physics VI*, volume 862 of *American Institute of Physics Conference Series*, pages 29–38, October 2006.

[93] H. K. Moffatt. *Magnetic Field Generation in Electrically Conducting Fluids*. CUP, New York, 1978.

[94] A. S. Monin and A. M. Yaglom, Statistical Fluid Mechanics, Vols 1 and 2, MIT Press Cambridge, Mass., 1971 and 1975).

[95] G. Joyce and D. Montgomery, "Negative temperature states for the two-dimensional guiding-centre plasma", J. Plasma Phys. **10**, 107 (1973).

[96] D. Montgomery, L. Turner, and G. Vahala, "Three-dimensional magnetohydrodynamic turbulence in cylindrical geometry." Phys. Fluids **21**, 757 (1978).

[97] D. Montgomery, L. Turner, and G. Vahala, "Most probable states in magnetohydrodynamics", **21**, 239 (1979).

[98] D. C. Montgomery, "Major Disruptions, Inverse Cascades, and the Strauss Equations ", Phys. Scripta, **T2**, 83 (1982).

[99] D. C. Montgomery, X. Shan, and W. H. Matthaeus. "Navier-Stokes relaxation to sinh-Poisson states at finite Reynolds numbers." *Phys. Fluids A*, **5**, 2207 (1993).

[100] D. Montgomery, W. H. Matthaeus, W. T. Stribling, D. Martinez, and S. Oughton, "Relaxation in two dimensions and the sinh-Poisson equation." Phys. Fluids A, **4**, 3 (1992).

[101] D. C. Montgomery and W. H. Matthaeus, "Oseen vortex as a maximum entropy state of a two dimensional fluid." Phys. Fluids, **23**, 075104 (2011).

[102] N. F. Ness, and L. F. Burlaga, "Spacecraft studies of the interplanetary magnetic field." J. Geophys. Res., **106**, 15803 (2001).

[103] M. Neugebauer, "Comment on the abundances of rotational and tangential discontinuities in the solar wind." J. Geophys. Res., **111**, A04103 (2006).

[104] M. Nelkin. "Universality and scaling in fully developed turbulence." *Adv. Phys.*, **43**, 143 (1994).

[105] S. Ohsaki and Z. Yoshida, "Variational principle with singular perturbation of hall magnetohydrodynamics." Phys. Plasmas, **12**, 064505 (2005).

[106] R.B. Pelz, V. Yakhot, S.A. Orszag, L. Shtilman and E. Levich, "Velocity-vorticity patterns in turbulent flow." Phys. Rev. Lett. **54**, 2505 (1985).

[107] K. T. Osman, W. H. Matthaeus, A. Greco, and S. Servidio, "Evidence for Inhomogeneous Heating in the Solar Wind", Astrophys. J., **727**, L11 (2011).

[108] K. T. Osman, M. Wan, W. H. Matthaeus, B. Breech, and S. Oughton, "Directional alignment and non-Gaussian statistics in solar wind turbulence." Astrophys. J, in press (2011).

[109] K. T. Osman, M. Wan, W.H. Matthaeus, J.M. Weygand, and S. Dasso, "Anisotropic third-moment estimates of the energy cascade in solar wind turbulence using multi-spacecraft data." Phys. Rev. Lett., in press (2011).

[110] S. Oughton, E. R. Priest, and W. H. Matthaeus, "The influence of a mean magnetic field on threedimensional magnetohydrodynamic turbulence.", J. Fluid Mech. **280**, 95 (1994).

[111] E. N. Parker. *Cosmical Magnetic Fields: Their Origin and Activity*. OUP, Oxford, UK, 1979.

[112] J. J. Podesta, "Dependence of solar-wind power spectra on the direction of the local mean magnetic field", Astrophys. J. **698**, 986 (2009).

[113] H. Politano and A. Pouquet, "Dynamical length scales for turbulent magnetized flows." Geophys. Res. Lett., **25**, 273 (1998).

[114] H. Politano, A. Pouquet, and V. Carbone, "Determination of anomalous exponents of structure functions in two-

dimensional magnetohydrodynamic turbulence." Europhys. Lett. **43**, 516 (1998).

[115] Y. Ponty, H. Politano, and J.-F. Pinton, "Simulation of Induction at Low Magnetic Prandtl Number", Phys. Rev. Lett., **92**, 144503 (2004).

[116] A. Pouquet, U. Frisch, and J. Léorat. "Strong MHD helical turbulence and the nonlinear dynamo effect." *J. Fluid Mech.*, **77**, 321 (1976).

[117] A. Pouquet, M. Meneguzzi, and U. Frisch. "Growth of correlations in magnetohydrodynamic turbulence." *Phys. Rev. A*, **33**, 4266 (1986).

[118] R. Robert and J. Sommeria, "Statistical equilibrium states for two-dimensional flows." *J. Fluid Mech.*, **229**, 291 (1991).

[119] R. Robert and J. Sommeria, "Relaxation towards a statistical equilibrium state in two-dimensional perfect fluid dynamics." *Phys. Rev. Lett.*, **69**, 2776 (1992).

[120] D. A. Roberts, L. W. Klein, M. L. Goldstein, and W. H. Matthaeus. "The nature and evolution of magnetohydrodynamic fluctuations in the solar wind: Voyager observations." *J. Geophys. Res.*, **92**, 11021 (1987).

[121] Roberts, D. A., M. A. Goldstein, W. H. Mettheeus, end S. Ghosh, "Velocity sheer generetion of soler wind turbulence." J. Geophys. Res., **97**, 17115 (1992).

[122] D. C. Robinson and M. G. Rusbridge. "Structure of turbulence in the zeta plasma." *Phys. Fluids*, bf 14, 2499 (1971).

[123] D. J., Rodgers, et al., "Hydrodynamic relaxation of an electron plasma to a near-maximum entropy state", Phys. Rev. Lett., **102**, 244501 (2009).

[124] D. J., Rodgers, W. H. Matthaeus, T. B. Mitchell, and D. C. Montgomery, "Similarity decay of enstrophy in an electron Fluid", Phys. Rev. Lett., **105**, 234501 (2010).

[125] A. A. Ruzmaikin, D. D. Sokoloff, and A. M. Shukurov "The dynamo origin of magnetic fields in galaxy clusters." Mon. Not. R. Astron. Soc. **241**, 1 (1989).

[126] Sahraoui, F., Goldstein, M. L., Robert, P., & Khotyaintsev, Y. V. 2009, Physical Review Letters, 102, 231102

[127] S. Servidio, W. H. Matthaeus, P. Dmitruk, "Depression of Nonlinearity in Decaying Isotropic MHD Turbulence", Phys. Rev. Lett. **100**, 095005 (2008).

[128] S. Servidio, W. H. Matthaeus, and V. Carbone, "Statistical properties of ideal three-dimensional Hall magnetohydrodynamics: The spectral structure of the equilibrium ensemble", Phys. Plasmas **15**, 042314 (2008).

[129] S. Servidio, W. H. Matthaeus, M. A. Shay, P. A. Cassak, P. Dmitruk, "Magnetic Reconnection in Two-Dimensional Magnetohydrodynamic Turbulence." Phys. Rev. Lett. **102**, 115003 (2009).

[130] S. Servidio, W. H. Matthaeus, P. Dmitruk, and V. Carbone Time decorrelation in isotropic magnetohydrodynamic turbuelnce, Europhysics Lett, in press (2011).

[131] A. Schalchi, Nonlinear Cosmic Ray Diffusion Theories, Astrophysics Space Science Library, vol. 362. Springer, Berlin (2009).

[132] J. V. Shebalin, W. H. Matthaeus, and D. Montgomery, "Anisotropy in MHD turbulence due to a mean magnetic field", J. Plasma Phys. **29**, 525 (1983).

[133] C. W. Smith, J. L'Heureux, N. F. Ness, M. H. Acuna, L. F. Burlaga, and J. Scheifele, "The ACE Magnetic Fields Experiment", Space Sci. Rev., **86**, 611 (1998).

[134] C. W. Smith, K. Hamilton, B. J. Vasquez, and R. J. Leamon . "Dependence of the Dissipation Range Spectrum of Interplanetary Magnetic Fluctuationson the Rate of Energy Cascade." *Astrophys. J.*, **645**, L85 (2006).

[135] L. Sorriso-Valvo, R. Marino, V. Carbone, A. Noullez, F. Lepreti, P. Veltri, R. Bruno, B. Bavassano, and E. Pietropaolo, "Observation of inertial energy cascade in interplanetary space plasma", Phys. Rev. Lett., **99**, 115001 (2007).

[136] L. Sorriso-Valvo, V. Carbone, P. Veltri, G. Consolini, and R. Bruno, "Intermittency in the solar wind turbulence through probability distribution functions of fluctuations." Geoph. Res. Lett., **26**, 1801 (1999).

[137] K. R. Sreenivasan, and R. A. Antonia, "The phenomenon of small-scale turbulence", Annu. Rev. Fluid Mech. **29**, 435 (1997).

[138] J. E. Stawarz, C. W. Smith, B. J. Vasquez, M. A. Forman, and B. T. MacBride, "The turbulent cascade and proton heating in the solar wind at 1 au." *Astrophys. J.*, **697**, 1119 (2009).

[139] H. R. Strauss. "Nonlinear, three-dimensional magnetohydrodynamics of noncircular tokamaks." *Phys. Fluids*, **19**, 134 (1976).

[140] Stribling and W. H. Matthaeus, "Statistical properties of ideal threedimensional magnetohydrodynamics", Phys. Fluids B **2**, 1979 (1990).

[141] T. Stribling and W. H. Matthaeus, "Relaxation processes in a low-order three-dimensional magnetohydrodynamics model", Phys. Fluids B, **3**, 1848 (1991).

[142] J. B. Taylor, "Relaxation of toroidal plasma and generation of reverse magnetic fields", Phys. Rev. Lett. **33**, 1139 (1974).

[143] J. B. Taylor, "Relaxation and magnetic reconnection in plasmas", Reviews of Modern Physics, **58**, 741 (1986).

[144] A. C. Ting, W. H. Matthaeus, and D. Montgomery. "Turbulent relaxation processes in magnetohydrodynamics." *Phys. Fluids*, **29**, 3261 (1986).

[145] B. T. Tsurutani and E. J. Smith, "Interplanetary discontinuities - Temporal variations and the radial gradient from 1 to 8.5 AU." J. Geophys. Res., **84**, 2773 (1979).

[146] B. J. Vasquez, C. W. Smith, K. Hamilton, B. T. MacBride, and R. J. Leamon, "Evaluation of the turbulent energy cascade rates from the upper inertial range in the solar wind at 1 AU", J. Geophys. Res., **112**, A07101 (2007).

[147] P. Veltri, and A. Mangeney, "Scaling laws and intermittent structures in solar wind MHD turbulence." Solar Wind IX, AIP Conference Proceedings, **471**, 543 (1999).

[148] P. Veltri, "MHD turbulence in the solar wind: self-similarity, intermittency and coherent structures." Plasma Phys. Control. Fusion, **41**, A787 (1999).

[149] A. Verdini, M. Velli, W. H. Matthaeus, S. Oughton, and P. Dmitruk, "A turbulence-driven model for heating and acceleration of the fast wind in coronal holes", Astrophys. J. Lett. **708**, L116 (2010).

[150] M. Wan, S. Oughton, S. Servidio, and W. H. Matthaeus, "Generation of non-Gaussian statistics and coherent structures in ideal magnetohydrodynamics", Phys. Plasmas, **16**, 080703 (2009).

[151] M. Wan, S. Oughton, S. Servidio, and W. H. Matthaeus, "von Karman self-preservation hypothesis for MHD turbulence and its consequences for universality", J. Fluid Mech. (submitted).

[152] J. M. Weygand, W. H. Matthaeus, M. El-Alaoui, S. Dasso, and M. G. Kivelson, "Anisotropy of the Taylor scale and the correlation scale in plasma sheet magnetic field fluctuations as a function of auroral electrojet activity", J. Geophys. Res. **115**, A12250 (2010).

[153] L. Woltjger, "A theorem on force-free magnetic fields", Proc. National Acad. Sci. USA, **44**, 489 (1958).

[154] N. Yokoi, R, Rubenstein, Hamba, Yoshizawa, A turbuelnce model for magnetohydrodynamic plasmas, Journal of Turbuelnce, 9, 1 (2008)

[155] A. Yoshizawa, Three equation modeling of inhomoge-

neous compressible turbulence based on a two-scale direct-interaction approximations, Phys. Fluids A, 2, 838 (1990)

[156] G. P. Zank and W. H. Matthaeus, "The equations of reduced magnetohydrodynamics", J. Plasma Phys. **48**, 85 (1992).

[157] G. P. Zank, S. Oughton, F. M. Neubauer, and G. M. Webb. "Properties of mass-loading shocks 2. Magnetohydrodynamics." *J. Geophys. Res.*, **97**, 17051 (1992).

[158] G. P. Zank, W. H. Matthaeus, and C. W. Smith. "Evolution of turbulent magnetic fluctuation power with heliocentric distance." *J. Geophys. Res.*, **101**, 17093 (1996).

[159] Y. Zhou and W. H. Matthaeus, "Transport and turbulence modeling of solar wind fluctuations", J. Geophys. Res. **95**, 10,291 (1990).

[160] Y. Zhou, W. H. Matthaeus, and P. Dmitruk. "Magnetohydrodynamic turbulence and time scales in astrophysical and space plasmas." *Rev. Mod. Phys.*, **76**, 1015 (2004).

[161] S. J. Zweben and R. J. Taylor, "Phenomenological comparison of magnetic and electrostatic fluctuations in the Macrotor tokamak." Nucl. Fusion, **21**, 193 (1981).

[162] D. R. Wells, Dynamic stability of closed plasma configurations, Journal of Plasma Physics, 4, 645 (1970).

[163] The unaveraged Alfvén timescale is $(\mathbf{k} \cdot \mathbf{B}_0)^{-1}$ where $\mathbf{B}_0$ is the mean magnetic field. This induces anisotropy [132] and the possibility of important additional time scale effects. Here we deal only with the isotropic case.